Global and Planetary Change 161 (2018) 10–27

Contents lists available at ScienceDirect

Global and Planetary Change

journal homepage: www.elsevier.com/locate/gloplacha

Mid-21st century projections of hydroclimate in Western Himalayas and Satluj River basin

Sarita Tiwari[a,b], Sarat C. Kar[a,*], R. Bhatla[b]

[a] National Centre for Medium Range Weather Forecasting, Noida, India
[b] Department of Geophysics, Banaras Hindu University, Varanasi, India

A B S T R A C T

The Himalayan climate system is sensitive to global warming and climate change. Regional hydrology and the downstream water flow in the rivers of Himalayan origin may change due to variations in snow and glacier melt in the region. This study examines the mid-21st century climate projections over western Himalayas from the Coupled Model Intercomparison Project Phase 5 (CMIP5) global climate models under Representative Concentration Pathways (RCP) scenarios (RCP4.5 and RCP8.5). All the global climate models used in the present analysis indicate that the study region would be warmer by mid-century. The temperature trends from all the models studied here are statistically significant at 95% confidence interval. Multi-model ensemble spreads show that there are large differences among the models in their projections of future climate with spread in temperature ranging from about 1.5 °C to 5 °C over various areas of western Himalayas in all the seasons. Spread in precipitation projections lies between 0.3 and 1 mm/day in all the seasons. Major shift in the timing of evaporation maxima and minima is noticed. The GFDL_ESM2G model products have been downscaled to Satluj River basin using the weather research and forecast (WRF) model and impact of climate change on streamflow has been studied. The reduction of precipitation during JJAS is expected to be > 3–6 mm/day in RCP8.5 as compared to present climate. It is expected that precipitation amount shall increase over Satluj basin in future (mid-21st century) The soil and water assessment tool (SWAT) model has been used to simulate the Satluj streamflow for the present and future climate using GFDL_ESM2G precipitation and temperature data as well as the WRF model downscaled data. The computations using the global model data show that total annual discharge from Satluj will be less in future than that in present climate, especially in peak discharge season (JJAS). The SWAT model with downscaled output indicates that during winter and spring, more discharge shall occur in future (RCP8.5) in Satluj River.

1. Introduction

It has been well documented that climate change is expected to have a strong impact on water resources, especially in mountain regions (Buytaert, 2012). In a regional scale, some of the noticeable impact would be rapid melting and reduction of glaciers leading to the increased magnitude of surface runoff (Beniston, 2003; Nogués-Bravo et al., 2007). The impact of climate change would be even more in the Himalayas where the rise in temperature, which is higher than the global average, has a significant effect on the cryosphere (Eriksson et al., 2009; IPCC, 2013). Several impact studies under climate change scenarios (Representative Concentration Pathways, RCPs) have been carried out over rivers basins located in different countries using outputs from the models of the Coupled Model Intercomparison Project Phase 5 (CMIP5 as well as other climate models (e.g. Christensen et al., 2004, Gosain et al., 2006 and Elshamy et al., 2009)).

Many studies have documented the impact of climate change over the Indian subcontinent considering temperature and precipitation projections (Chaturvedi et al., 2012; Pattnayak et al., 2013; Dash et al., 2014). Chaturvedi et al. (2012) noted that temperatures will increase from of 2 °C (RCP2.6) to 4.8 °C (RCP8.5) over India from 1880s to 2080s. It is projected that the all-India precipitation will increase by 6% to 14% under various RCP scenarios from the base climate. Sengupta and Rajeevan (2013) have examined the CMIP5 simulated results over the Indian region in detail and have ranked these models in terms of skill of precipitation and temperature simulations. Pattnayak et al. (2017) have examined output from several CMIP5 global models and concluded that the signals of rate of increase or decrease in precipitation and temperature over the countries nearing the Bay of Bengal are stronger in RCP8.5 than that in RCP4.5. However, no such studies exist

* Corresponding author at: National Centre for Medium Range Weather Forecasting, A-50, Sector-62, Noida, India.
E-mail address: sckar@ncmrwf.gov.in (S.C. Kar).

https://doi.org/10.1016/j.gloplacha.2017.10.013
Received 31 March 2017; Received in revised form 25 September 2017; Accepted 25 October 2017
Available online 02 December 2017
0921-8181/ © 2017 Elsevier B.V. All rights reserved.

Table 1
List of CMIP5 climate models used in this study.

Models	Modelling centre/group	Resolution (Lat × Lon)	Simulation period	Reference
GFDL_ESM2G	NOAA Geophysical Fluid Dynamics Laboratory, USA	2.0° × 2.5°	2001–2060	Dunne et al. (2013)
GFDL_ESM2M	NOAA Geophysical Fluid Dynamics Laboratory, USA	2.0° × 2.5°	2001–2060	Dunne et al. (2013)
GISS_E2_H	NASA Goddard Institute for Space Studies, USA	2.0° × 2.5°	2001–2060	Schmidt et al. (2014)
HadGEM2_AO	Met Office, Hadley Centre, UK	1.25° × 1.875°	2001–2060	Martin et al. (2011)
HadGEM2_CC	Met Office, Hadley Centre, UK	1.25° × 1.875°	2001–2060	Martin et al. (2011)
HadGEM2_ES	Met Office, Hadley Centre, UK	1.25° × 1.875°	2001–2060	Collins et al. (2011)
MIROC_ESM	JAMSTEC, AORI and NIES, Japan	2.81° × 2.81°	2001–2060	Watanabe et al. (2011)

for the western Himalayan region.

Very little work has been carried out in India on the impact of climate change on hydrology (Divya and Mehrotra, 1995). The major river systems of the Indian subcontinent, which originate in the Himalayas, are expected to be more vulnerable to climate change because of the substantial contribution from snow and glaciers into these river systems (Nogués-Bravo et al., 2007). Snow in the Himalayan region is often close to its melting point. Therefore, any minor changes in temperature would affect snowmelt process rapidly. Due to global warming in the future, regions experiencing snowfall will increasingly experience precipitation in the form of rain. Beniston (2003) has noted that for every °C increase in temperature, the snowline will rise by about 150 m. It is also seen that shifts in snow-pack duration and amount due to sustained climate change will crucially affect water availability. The temperature rise and associated reduction of precipitation in recent few decades in the western Himalayan region have been studied by Bhutiyani et al. (2007, 2010). The hydrological response of these changes indicates reduction of stream flow in most of the western Himalayan Rivers (Thayyen and Gergan, 2010; Bhutiyani et al., 2008). Singh and Bengtsson (2004) have studied the impact of climate on melt and evaporation for the rain-fed, snow-fed and glacier-fed basins in the Himalayan region and suggested that snow-fed basins are more sensitive in terms of reduction in water availability in a warming climate. Immerzeel et al. (2013) have found that contrary to the climate response during the past three decades, the CMIP5 climate models predict increase in precipitation over many of the river basins in the western Himalayas which would lead to increased streamflow through the current century. In a warmer world, a shift in peak river runoff to winter and early spring is expected (Barnett et al., 2005).

Satluj is one of the important rivers for the Indian subcontinent with its origin in Himalayas. The river discharge depends on snowmelt as well as rainfall runoff. Singh and Kumar (1997) have investigated the effect of climate change on the snow water equivalent, snow/glacier melt runoff total streamflow and their distribution for the Spiti River, tributaries of the Saluj River. Tiwari et al. (2015, 2016a) have made a detailed examination of interannual variability of snowfall, snow accumulation and snowmelt in Satluj river basin.

Limitations of the global climate models in resolving physical processes such as cloud/convection and land-surface processes in local to regional scales become far more important especially in regions with topography such as the Himalayas (Wilby et al., 2004, Randall et al., 2007 and Fowler et al., 2007) and have described how the coarse resolution GCMs are insufficient for detailed assessment of climate change impacts at local or regional scales. Several downscaling methodologies have been developed to represent the sharp physiographic features of mountain areas in regional climate models (Tiwari et al., 2016b; Tiwari et al., 2017a).

From the foregoing discussion, it is found that no detailed study on the projected climate for the future has been undertaken so far for the western Himalayan region. The results of global climate models have not been downscaled to river basin scale. Moreover, snowmelt runoff models and the future climate data have not yet been used for Satluj River. Therefore, the main objective of the present work is to reduce these knowledge gaps. Mid-21st century projections of seven CMIP5 models have been examined for the western Himalayan region. Products of one GCM have been downscaled using the Weather Research and Forecast (WRF) model and simulated products have been used to force a snowmelt runoff model (Soil and Water Assessment Tool, SWAT) to simulate discharge of Satluj River in mid-21st century. The models, data used, analysis methodology as well as downscaling experiments are presented in Section 2. The global model results are provided in Section 3. The results from downscaling runs are described in Section 4. Section 5 has the application of projected hydroclimate data on the streamflow projections in Satluj River. The study is concluded in Section 6.

2. Data, model and methodology

2.1. Data used

Among the available CMIP5 model simulations, seven models have been chosen to analyze the present-day (historical) and projected climate in RCP 4.5 and 8.5. Moss and Edmonds (2010) have assigned priority to the RCPs. The highest emission scenario RCP8.5 is the first priority and the scenario with stabilization without overshoot i.e. RCP4.5 is the second priority. Thus, these two scenarios have been selected for this study. The climate models used in this study are listed in Table 1, together with their host institutions, and their abbreviations as used in this study. Availability of the model projections for dynamic downscaling has been one of the criteria for selecting the models for the present study. Data compiled by Climate Research Unit (CRU) of East Anglia, UK have been used for observations. CRU surface temperature (Ts) and precipitation at 0.5° × 0.5° (Harris et al., 2014) for the period 1901 to 2012 are used in the present study. Observing stations in the inaccessible area of western Himalayas are few. Although, in recent years, few high-quality observing stations have been setup, the observational information provided by station data in this area remains extremely uneven and nonhomogeneous. Harris et al. (2014) and references there-in, have described various data sources used in preparing the CRU data. New et al. (2000) have provided the distribution of temperature and precipitation stations used in its preparation. It may be noted that in the study region, at least 5 number of stations exist in a 5° × 5°°grid box for temperature (Jones et al., 2012). Mitchel and Jones (2005) have described the elaborate procedure for homogenization of data and merging the data from various sources. New et al. (2001) has reviewed the existing precipitation data sets and analysed the information about precipitation trends and variability on a global perspective. Precipitation stations in the study region are more, however, the rain gauge network covers mainly valleys and lowland areas. This may lead to a bias toward the lower elevations in the observations. The APHRODITE temperature data are available only for the period of 1973–2007. Observing station data from India Meteorological Department (IMD) are only available for the region within the Indian boundary. Palazzi et al. (2013) have compared precipitation in the Hindu-Kush Karakoram Himalaya from various sources. Therefore, while, the CRU data for temperature and precipitation have been

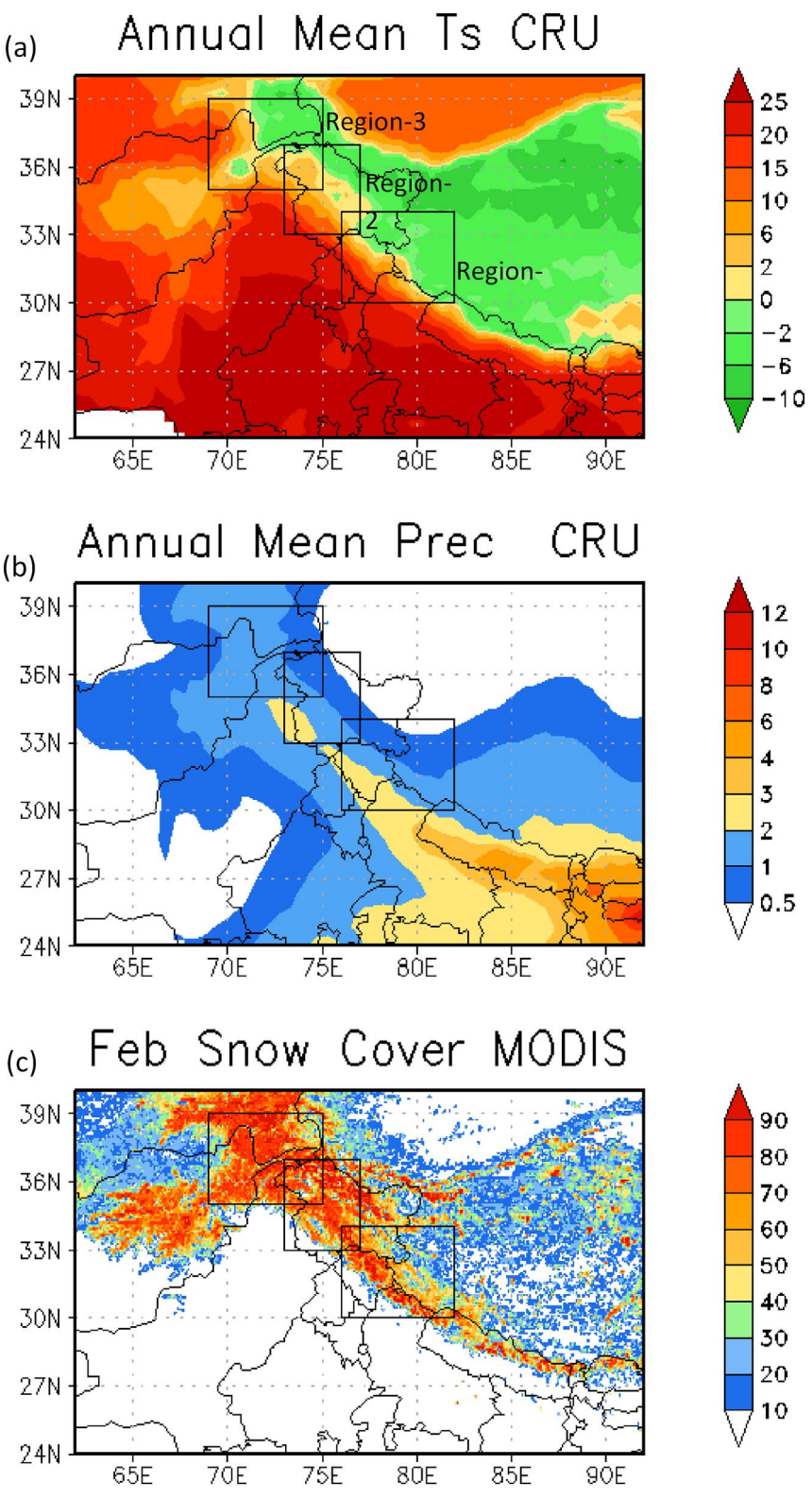

Fig. 1. Annual mean (averaged over the period 1901 to 2012) of (a) observed surface temperature (Ts, °C), (b) observed precipitation (mm/day) from CRU and (c) snow cover (%) in February (averaged over the period 2002 to 2014 derived from MODIS data. The three regions (Region-1, Region-2 and Region-3) used in the study are marked in figures as rectangular boxes.

prepared using observed data from various sources, there are large uncertainties in the representation of hydroclimate in the western Himalayan region in this data. Nevertheless various studies have used CRU data to explain the present climatic trend in the region. Monthly MODIS snow cover data (Hall et al., 2006) at 0.05° × 0.05° has also been used in the present study which has been downloaded from www.nsidc.org.

2.2. WRF model configuration

For downscaling purpose, the weather research and forecasting (WRF) model version 3.7.1 (Skamarock et al., 2005) has been used in the present study. The microphysics scheme is the WSM6-class scheme (Hong and Lim, 2006). The convection scheme used for these simulation runs is Grell-Devenyi scheme (Grell and Devenyi, 2002). The

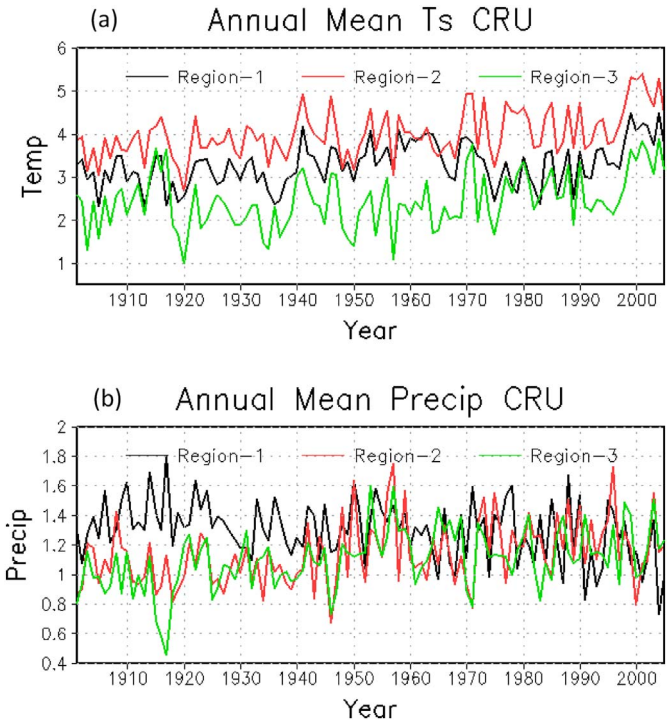

Fig. 2. Interannual variations of area averaged (a) temperature and (b) precipitation from 1901 to 2005. The three regions are marked in Fig. 1.

NOAH land-surface model (Chen and Dudhia, 2000) with 4-layers of soil and Yonsei University (YSU) planetary boundary layer (PBL) parameterization schemes (Hong and Pan, 1996) have been used in the present study.

Tiwari et al. (2017b) have carried out dynamic downscaling runs using various combinations of physical parameterization schemes for the western Himalayan region as in the present study. The two schemes (namely WSM6 for microphysics and Grell-Devenyi for convection) were found to produce more realistic results. In the present study, three sets simulations have been carried out using initial and boundary conditions from the GFDL_ESM2G model. Downscaling run with historical forcing is carried out for 2001 to 2005. GFDL_ESM2G model projections for 2051 to 2055 from RCP4.5 and RCP8.5 scenarios have also been used. In the present study, three nested domains with resolutions of 72 km, 24 km and 8 km have been designed. There are two strategies for dynamic downscaling using the WRF model (Lo et al., 2008). One may follow long-term continuous integration of the model starting with one initial condition and updating boundary conditions or by consecutive integration with frequent re-initialization. In the present study the second approach was adopted. For every experiment, the WRF model was run for 7-days each starting from initial conditions spaced every five days. The first 2-days of simulation outputs from every run are not used in the analysis as initial 48-h period is considered as a spin-up time of the model.

Trend in a time series detects that whether that parameter has any positive or negative increment with time or no change with time. Generally Mann-Kendall non parametric test is used for identification of trend in time series of hydrological parameter. The issue of stationarity is important for water resources engineering and management (Milly et al., 2008). While all the observed variations in the hydroclimatic processes can be represented with stationary stochastic models, it is important to examine the trend and stationarity in hydrological time series. The stationarity in hydroclimate data has been established in this study using augmented Dickey–Fuller (ADF) test (Dickey and Fuller, 1979) and Kwiatkowski–Phillips–Schmidt–Shin (KPSS) test (Kwiatkowski et al., 1992).

3. Global model results

3.1. Present climate

The Indian hydroclimate is dominated by the monsoon precipitation during June to September and precipitation (snowfall and rainfall) during December to March in the northern parts of India (Himalayas). Fig. 1a shows the annual mean observed surface temperature averaged over the period 1901 to 2012 from CRU over northern parts of India and adjoining Himalayas. While the higher reaches of the Himalayas experience negative annual mean temperatures, the plains of northern India have temperature > 20 to 25 °C. A sharp gradient in temperature is noticed over the foothills of Himalayas. Annual mean precipitation

Table 2
Linear regression equation and temperature and precipitation trend under from observed CRU data and model simulations.

Regions	Model names	Parameters			
		Precipitation		Temperature	
		R^2	Regression equation	R^2	Regression equation
Region-1	CRU	0.1108	y = −0.0022x + 1.413	0.1428	y = 0.0062x + 2.9549
	GFDL_RCP45	0.0677	y = −0.0053x + 0.1262	0.4312	y = 0.0238x + 0.3059
	GFDL_RCP85	0.0013	y = 0.0008x − 0.0659	0.4741	y = 0.0358x + 0.2649
	Hadgem2_RCP45	0.0364	y = 0.0039x − 0.101	0.7644	y = 0.041x + 0.0465
	GISS_RCP45	2.E-06	y = −3E − 05x + 0.0842	0.6639	y = 0.034x + 0.6225
	MIROC_RCP45	0.0299	y = 0.0052x − 0.1102	0.6447	y = 0.0519x + 0.2114
Region-2	CRU	0.1254	y = 0.0025x + 1.0073	0.2278	y = 0.0086x + 3.5531
	GFDL_RCP45	0.0012	y = −0.0007x + 0.0542	0.541	y = 0.0377x + 0.3766
	GFDL_RCP85	0.0873	y = 0.008x − 0.148	0.581	y = 0.0459x + 0.4511
	Hadgem2_RCP45	0.0422	y = 0.0036x − 0.0529	0.7722	y = 0.0378x + 0.0819
	GISS_RCP45	0.0003	y = −0.0004x + 0.0483	0.6013	y = 0.0343x + 0.7883
	MIROC_RCP45	0.0006	y = 0.0006x + 0.0494	0.664	y = 0.0573x + 0.0075
Region-3	CRU	0.1886	y = 0.0029x + 0.9494	0.113	y = 0.007x + 2.0752
	GFDL_RCP45	0.0231	y = 0.0025x − 0.0608	0.5913	y = 0.0379x + 0.2727
	GFDL_RCP85	0.0579	y = 0.0046x − 0.1174	0.6125	y = 0.0567x + 0.1431
	Hadgem2_RCP45	0.0378	y = 0.0029x + 0.0345	0.7467	y = 0.0419x + 0.0793
	GISS_RCP45	0.0147	y = −0.0028x + 0.1418	0.5434	y = 0.033x + 0.7577
	MIROC_RCP45	0.0104	y = −0.0019x + 0.0995	0.6231	y = 0.0533x + 0.0118

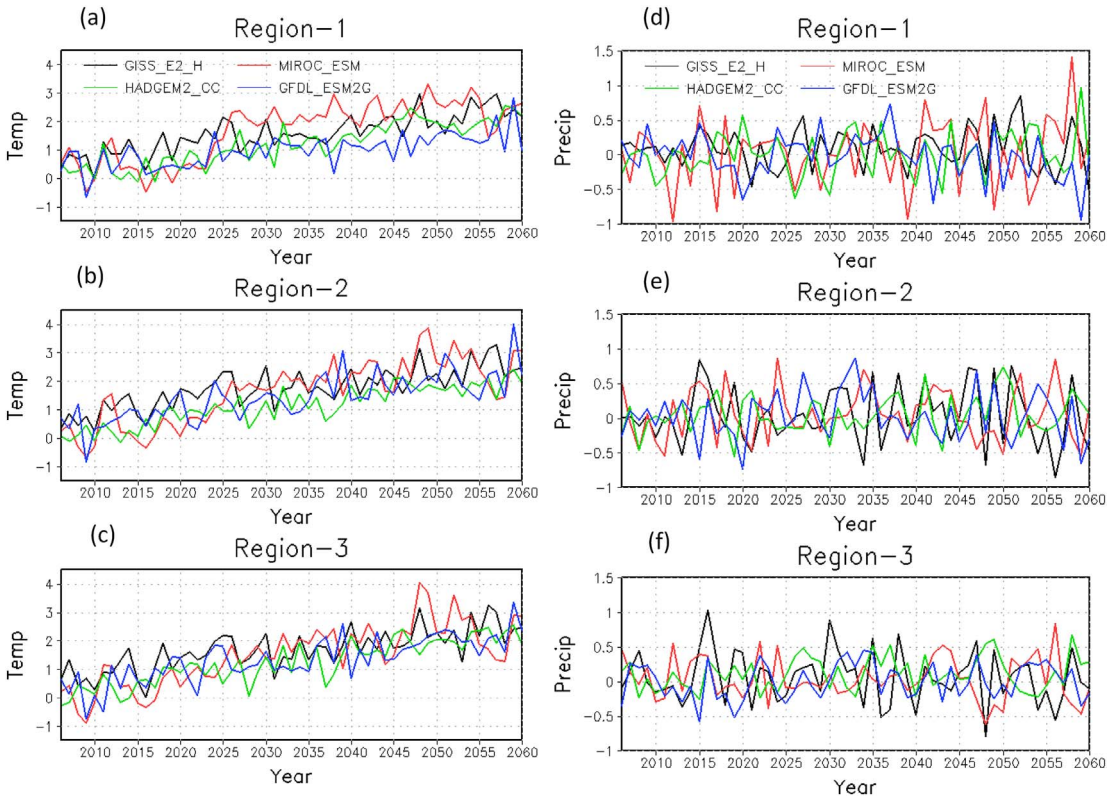

Fig. 3. Temperature and precipitation trends in various models in RCP4.5 scenario from 2006 to 2060: temperature trend (a) Region-1; (b) Region-2 and (c) Region-3; precipitation trend (d) Region-1; (e) Region-2 and (f) Region-3.

Table 3
Mann-Kendall analysis of trend of GFDL_ESM2G model projections of temperature and precipitation under RCP4.5 and RCP8.5 scenarios.

	Parameter	Scenario	Tau	p-Value (one-tailed)
Region-1	Temperature	RCP4.5	0.481	< 0.0001
	Temperature	RCP8.5	0.476	< 0.0001
	Precipitation	RCP4.5	− 0.153	0.950
	Precipitation	RCP8.5	0.021	0.414
Region-2	Temperature	RCP4.5	0.582	< 0.0001
	Temperature	RCP8.5	0.564	< 0.0001
	Precipitation	RCP4.5	− 0.038	0.658
	Precipitation	RCP8.5	0.231	0.007
Region-3	Temperature	RCP4.5	0.578	< 0.0001
	Temperature	RCP8.5	0.600	< 0.0001
	Precipitation	RCP4.5	0.087	0.176
	Precipitation	RCP8.5	0.166	0.037

over the region for the same period is shown in Fig. 1b. A north-west south-east precipitation band along the Himalayas is noticeable. The Gangetic plain and parts of north-east India have precipitation ranging to > 8–10 mm/day, mostly contributed by monsoon precipitation during JJAS months. Snow cover area (%) from MODIS satellite for the month of February averaged over the period 2002 to 2014 is shown in Fig. 1c. Snow cover over the Indian parts of Himalayas is characterized by a north-west south-east band. Over Afghanistan, Karakorum region and adjoining regions are mostly covered by snow in February.

Interannual variations of area averaged temperature and precipitation from 1901 to 2005 are shown in Fig. 2a and b for temperature and precipitation respectively. The regions are Region-1, Region-2 and Region-3 as marked in Fig. 1. The longitudinal and latitudinal extents of these regions are Region-1: between 76°E to 82°E and 30°N to 34°N; Region-2: between 73°E to 77°E and 33°N–37°N and Region-3 between 69°E to 75°E and 35°N to 39°N. While Region-1 is surrounding Satluj river basin in Himachal Pradesh and neighbouring Tibet, Region-2 corresponds to western parts of Kashmir and adjoining region. Region-3 represents a part of northern Kashmir along with the region north of that. Considerable interannual variations are noticed in both precipitation and temperature in all the three regions. While Region-3 is the coldest region (due to topography influence), Region-2 is the warmest. However, in recent decades, an increase in annual mean temperature is noticed, especially for Region-2 and Region-3. In order to examine if any trend exists, temperature differences for two 30 year periods (1946 to 1975 and 1976 to 2005) have been computed. It is found that Region-1 has cooled by about 0.117 °C in the recent 30-year period. However, temperature has risen by 0.415 °C in Region-2 and 0.553 °C in Region-3. Therefore, it is found that climate of the region surrounding Satluj River basin is different from other two regions. Area averaged precipitation for the three regions are not very different except that Region-1 used to experience more precipitation from 1901 to 1940 than other two regions. It is also noticed that there is no large trend in precipitation. The difference in precipitation between two 30-year periods indicates that the amount of precipitation has fallen by 0.08 mm/day in Region 1 and 0.016 mm/day in Region-3. In Region-2 precipitation amount has increased by 0.042 mm/day. The linear trend line equations for the CRU temperature and precipitation from 1901 to 2005 are provided in Table 2 along with their respective R^2 values. A marginal warming trend is noticed in the trend line. However, R^2 values for all the three regions is too low (< 20%). Similar trend lines for precipitation indicate a marginal reducing trend in Region-1 and marginal increasing trend in the Region-2 and Region-3.

3.2. Projected climate

Annual mean surface air temperature projections of future climate (from 2006 to 2060) in RCP4.5 scenario from four climate models are

Table 4
ADF and KPSS test results of stationarity analysis of GFDL_ESM2G model projections of temperature and precipitation under RCP4.5 and RCP8.5 scenarios.

	Parameter	Model	ADF test		KPSS test	
			Tau	p-Value (one-tailed)	Eta	p-Value (one-tailed)
Region-1	Temperature	RCP4.5	− 3.524	0.043	0.040	0.815
	Temperature	RCP8.5	− 2.141	0.505	0.267	0.001
	Precipitation	RCP4.5	− 2.423	0.355	0.159	0.034
	Precipitation	RCP8.5	− 3.038	0.123	0.098	0.185
Region-2	Temperature	RCP4.5	− 5.157	0.001	0.029	0.953
	Temperature	RCP8.5	− 2.723	0.222	0.164	0.029
	Precipitation	RCP4.5	− 3.619	0.034	0.117	0.110
	Precipitation	RCP8.5	− 2.964	0.143	0.149	0.046
Region-3	Temperature	RCP4.5	− 4.619	0.003	0.047	0.712
	Temperature	RCP8.5	− 2.944	0.149	0.166	0.027
	Precipitation	RCP4.5	− 3.651	0.032	0.073	0.368
	Precipitation	RCP8.5	− 3.540	0.042	0.098	0.188

shown in Fig. 3(a, b, c) respectively for Region-1, Region-2 and Region-3. The four climate models chosen for this analysis are GFDL_ESM2G, GISS_E2_H, HADGEM2_CC and MIROC_ESM. The trends in this analysis are based on annual mean temperature for a 30-year period from 1975 to 2005 of their respective historical climate simulations. It is seen that for all the three regions, an increasing trend exists for all the models. However, different models behave differently over these regions with differences in warming amount and interannual variability. The GFDL_ESM2G model projects less warming for Region-1 after 2030 than other models. For this region, MIROC_ESM has maximum warming especially after 2020. Annual mean precipitation projections of future climate (from 2006 to 2060) in RCP4.5 scenario from four climate models are shown in Fig. 3(d, e, f) respectively for Region-1, Region-2 and Region-3. No noticeable trend is seen from any model or for any region. Large interannual variations in precipitation change are seen in MIROC_ESM. The GFDL_ESM2G model projects less precipitation change from 2050 to 2060. The linear trend line equations for the four models from 2006 to 2060 for temperature under RCP4.5 scenario are provided in Table 2 along with their respective R^2 values. In addition, linear trend line equation for GFDL-ESM2G model under RCP8.5 scenario has also been provided for comparison purpose. Increasing temperature trend in GFDL_ESM2G model projections is minimum for Region-1 while, the MIROC_ESM has the maximum warming trend. The GFDL_ESM2G model projects that the decade from 2051 to 2060 for Region-1 would be about 1.0 °C warmer than the other two regions. The MIROC_ESM model projects that this decade would be about 3 °C warmer in all the regions than the present climate. The HADGEM2_CC, GISS_E2_H and MIROC_ESM models project almost a linear trend starting from 2006 to 2060 with higher values of R^2 for all the three regions. Therefore, all the models used in the present analysis indicate that in RCP4.5 scenario, all the three regions would be warmer. Similar analysis has been carried out for examining precipitation trend as shown in Table 2. It is found that precipitation has large interannual variation as well as large inter-model variation. No linear trend is

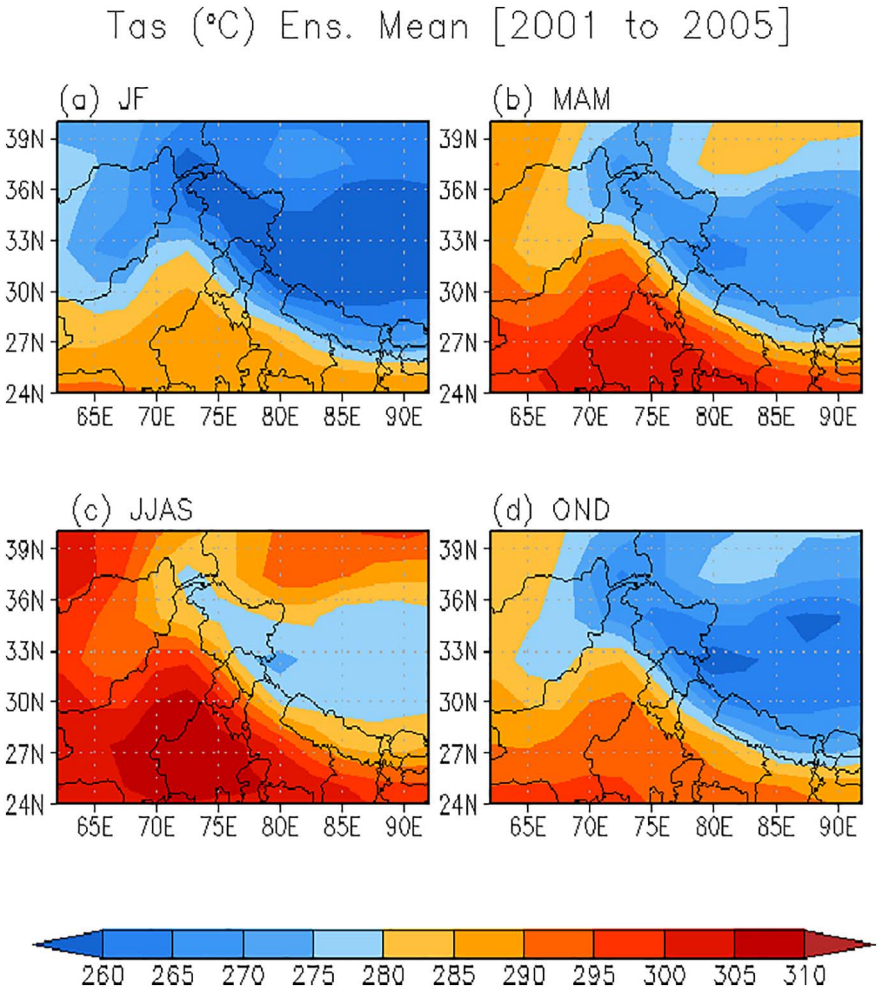

Fig. 4. Multi-model ensemble means temperature simulations (averaged over 2001 to 2005) for (a) January February (JF), (b) March to May (MAM), (c) June to September (JJAS) and (d) October to December (OND).

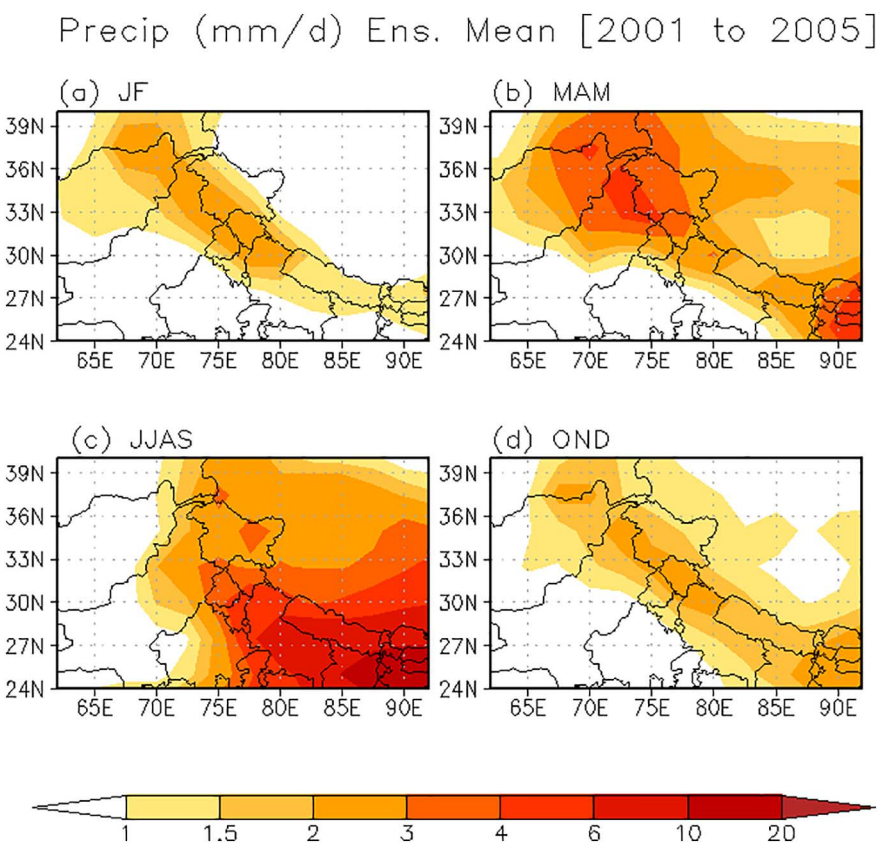

Fig. 5. Same as Fig. 4, but for precipitation (mm/day).

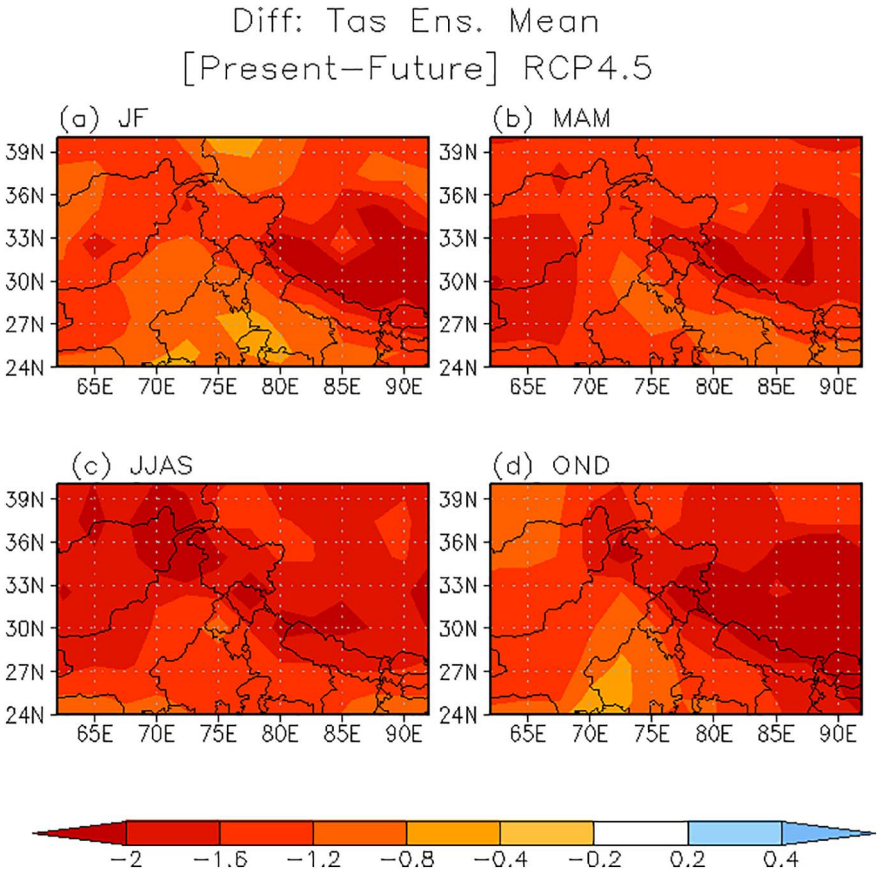

Fig. 6. Multi-model ensemble mean difference in surface air temperature (°C) between present climate (2001–2005) and mid-21st century projections (2051–2055) in RCP4.5 scenario (a) January February (JF), (b) March to May (MAM), (c) June to September (JJAS) and (d) October to December (OND).

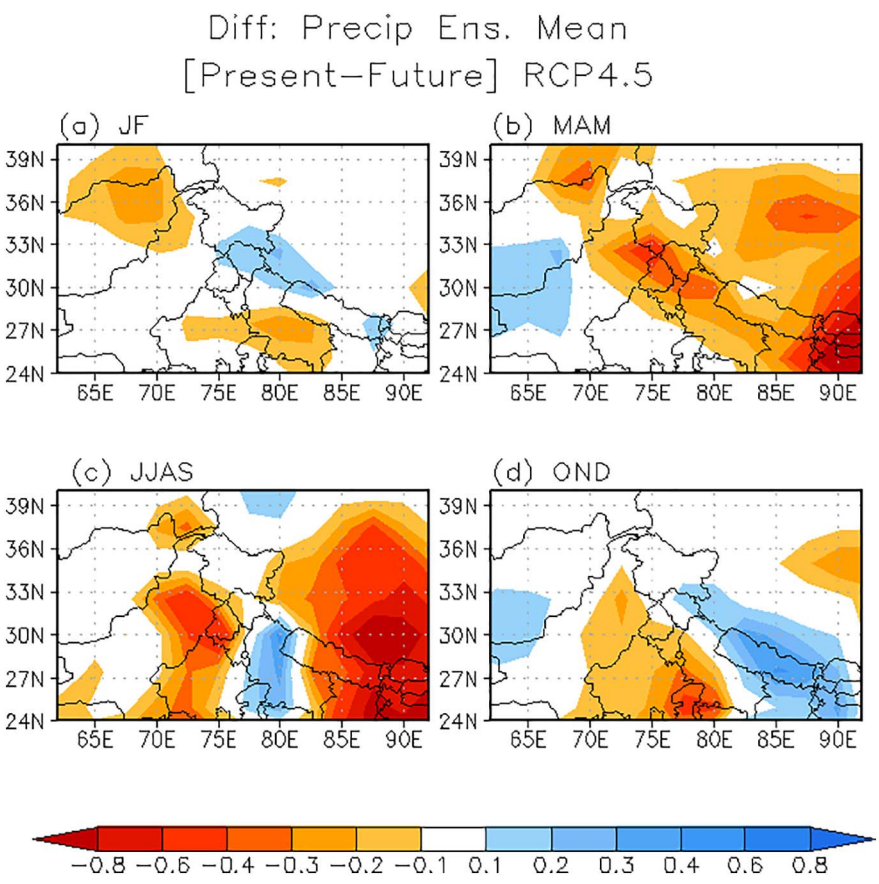

Fig. 7. Same as Fig. 6, but for precipitation (mm/day).

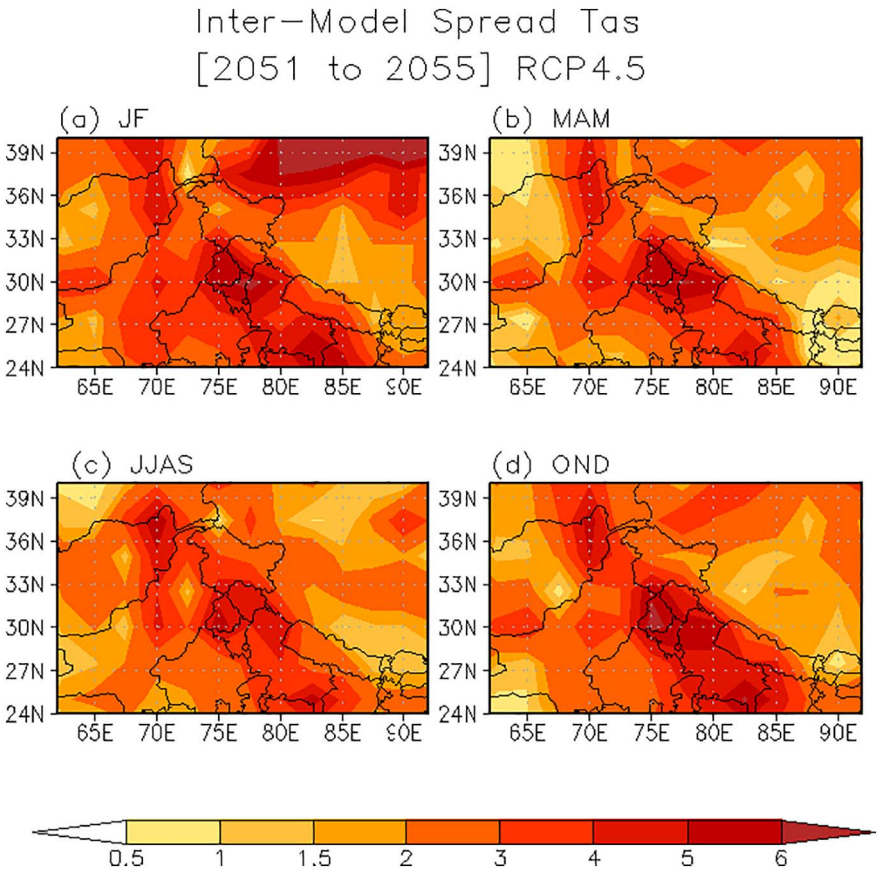

Fig. 8. Inter-model ensemble spread for surface air temperature (°C) in mid-21st century projections (2051–2055) in RCP4.5 scenario (a) January February (JF), (b) March to May (MAM), (c) June to September (JJAS) and (d) October to December (OND).

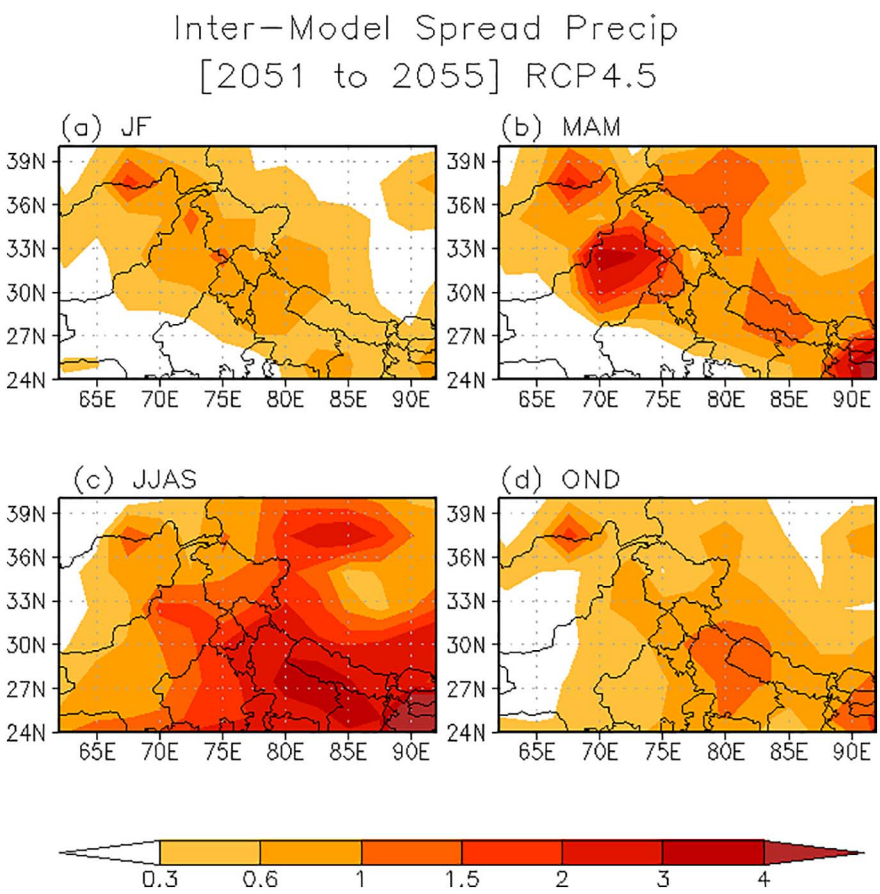

Fig. 9. Same as Fig. 8, but for precipitation (mm/day).

noticed in case of all the models and all the regions. Spatial patterns of temperature and precipitation changes have been analysed in further detail and discussed later.

3.3. Trend and stationarity analysis

Statistical significance of the climate change assessment from model simulations for both temperature and precipitation has been tested. Mann Kendal test has been applied on the model simulation data of 60 years period (2000–2060) to establish the statistical significance of the trend. It is found that all the temperature trends from all the models studied here are statistically significant. As the GFDL_ESM2G model has the least trend among all, a detailed trend analysis for this model is presented here. The trend analysis results for this model are provided in Table 3. Similar trend values are obtained for all the three regions as marked in Fig. 1. It is seen that the increasing trend in future climate data of temperature under both the scenarios is significant at 95% confidence interval as the p-values are less than significant level (0.05). The trend in precipitation is not significant for either the RCP4.5 and in RCP8.5. In all the three regions, a statistically significant increasing trend in temperature is obtained while for precipitation, the trend is not significant.

Stationary test determines whether mean values and variance of a time series vary with time. It may be noted that all the techniques of time series analysis assume that there is some kind of stationarity in the series. Therefore, it is necessary to first test the stationarity for justification of using a model. In the present study, stationarity test has been carried out using two methods: (i) augmented Dicky-Fuller (ADF) unit root test and (ii) KPSS test. The test results are shown in Table 4. ADF unit root test was first proposed by Dickey and Fuller (1979). This test identifies the presence of unit roots in the series. KPSS test was performed first by Kwiatkowski et al. (1992) and tests the trend stationarity. GFDL_ESM2G model data for RCP4.5 and RCP8.5 scenarios have been chosen to carry out the analysis. In the ADF test, if the calculated tau value is less than the critical value in the table of critical values (-0.743 in the present case), then a significant result is obtained; otherwise the null hypothesis is accepted that there is a unit root and the time series is not stationary. It is seen in the present analysis that in all the three regions, there is stationarity with 95% confidence interval in temperature and precipitation time series for this model. However, the results are different for the three regions and for two scenarios considered in the present study. Similar conclusion is also obtained with the KPSS test that the temperature time series is trend stationary at 95% confidence interval.

3.4. Spatial patterns of multi-model mean

Spatial patterns of surface air temperature (Tas) and precipitation for the period 2001 to 2005 have been examined from multi-model ensemble mean. The models considered are GFDL_ESM2G, GFDL_ESM2M, HADGEM2_AO, HADGEM2_CC, HADGEM2_ES, MIROC_ESM and GISS_E2_H. Ability of these models and their ensemble mean to simulate the present climate using historical forcing has been highlighted. Knutti et al. (2010) have examined the issues and challenges in combining projections from multiple climate models. Fig. 4(a–d) show five-year mean of temperature simulations from ensemble mean for January February (JF), March to May (MAM), June to September (JJAS) and October to December (OND) respectively. All the models simulate colder temperatures over the Himalayas in JF. The area of colder temperature (< 280 K) shrinks when one progresses from JF to MAM and JJAS. This area further increases in OND as fall and winter season begins. Even though, these models have rather coarse

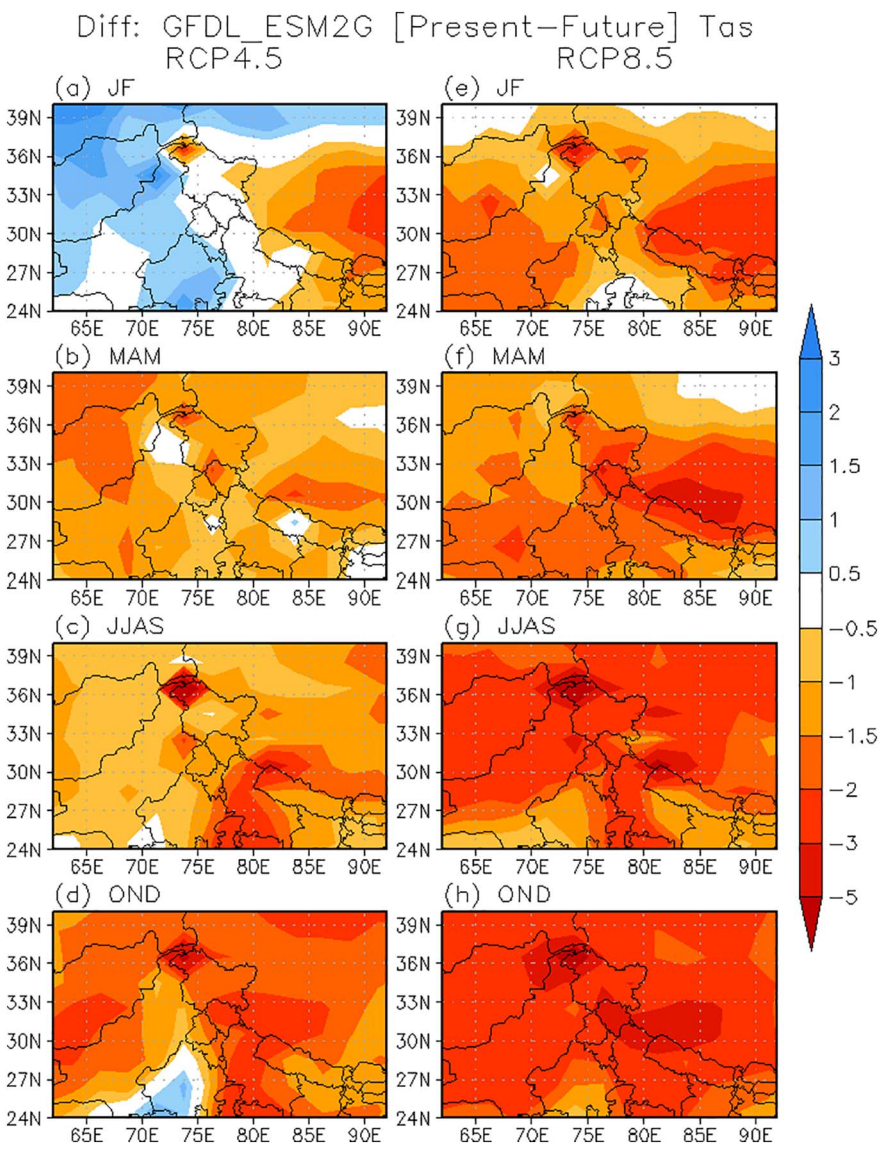

Fig. 10. Difference in surface air temperature (°C) between present climate (2001–2005) and mid-21st century projections (2051–2055) for the GFDL_ESM2G model (a) January February (JF), (b) March to May (MAM), (c) June to September (JJAS) and (d) October to December (OND) in RCP4.5 scenario; (e) January February (JF), (f) March to May (MAM), (g) June to September (JJAS) and (h) October to December (OND) in RCP8.5 scenario.

horizontal resolutions, the models are able to simulate the sharp gradient in temperature along the foothills of Himalayas as observed. Spatial patterns of precipitation have been simulated well by the models as seen in the ensemble plots of JF, MAM, JJAS and OND in Fig. 5(a–d) respectively. The ensemble mean clearly depicts a north-west-southeast oriented precipitation band over Jammu and Kashmir, Himachal Pradesh and Uttarakhand regions. Large amount of precipitation simulated by the models in MAM over northern parts of Kashmir, Pakistan and Afghanistan may be unrealistic. In JJAS, the monsoon precipitation over the Gangetic plain is also simulated well. Therefore, it can be said that the ensemble mean of simulations of temperature and precipitation with historical forcing for the period 2001–2005 are reasonable.

Mid-21st century projections (2051–2055) of the climate (difference from the base period of 2001–2005) have been examined from the ensemble mean of model projections in RCP4.5 scenario. The plots for surface air temperature (Tas) are shown in Fig. 6(a–d) and similar plots for precipitation are shown in Fig. 7(a–d) for JF, MAM, JJAS and OND respectively. In JF, temperature rise would be from 0.2 to 0.8 °C over most parts of northern India plains. Over the Himalayan parts of Kashmir, Himachal and Uttarakhand, the rise in temperature will be from 0.8 to 1.6 °C in all the seasons except JJAS when the temperature rise is expected to be about 1.6 to 2 °C. Except in JJAS months, a north-south gradient in temperature rise is noticed with the Himalayan region experiencing warmer temperatures as compared to present climate simulations with historical forcing. In JF, no large difference in precipitation is seen in ensemble mean simulations during 2051–2055. In MAM, the models indicate an increase in precipitation (0.4 to 0.6 mm/day) in north India and the Himalayas. During JJAS, it is projected that the central and eastern Himalayan region will get more precipitation (> 0,8 mm/day) in some areas. No large change in and around Satluj River basin may occur. A marginal reduction in precipitation (0.2 to 0.4 mm/day) is expected in OND over the study region including regions close to foothills of Himalayas.

As is seen in Figs. 4 and 5, there are large differences among the models in their projections of future climate. In order to examine the spatial distribution of this inter-model spread and to document the uncertainties in the projections, the spread for Tas and precipitation for the four seasons are shown in Figs. 8(a–d) and 9(a–d) respectively. It is seen that there are large uncertainties in the temperature projections around Punjab, Himachal and Uttarakhand regions. These uncertainties exceed even 5 °C in some areas. In JJAS, the intermodal spread is about 3 to 4 °C. While the neighbouring regions of Tibetan Himalayas have spread of about 1.5 to 2 °C, it is important to note that the neighbouring

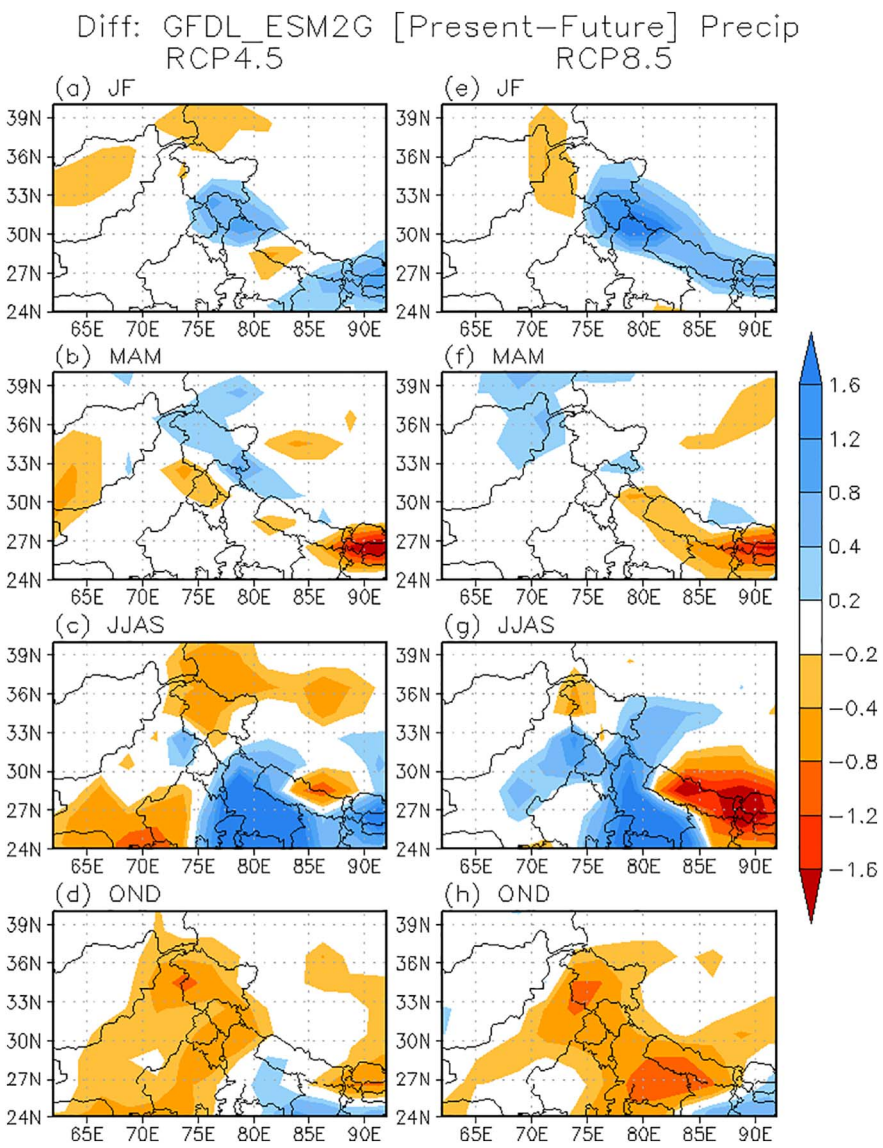

Fig. 11. Same as Fig. 10, but for precipitation (mm/day).

Satluj basin has large uncertainties in temperature projections (3 to 5 °C). In ensemble mean, where all the model projections are combined using same weights, any single model having large amplitude of change would dominate the ensemble mean. Spread in the precipitation projections lies between 0.3 and 1 mm/day in all the seasons except in JJAS when the spread is > 3 mm/day along the Gangetic plains and foothill regions. Tiwari et al. (2014) have discussed the global model simulation skill for winter season from several global models and found that the models have difficulty in simulating seasonal mean precipitation over the region even one season in advance. Moreover, it is found in the present study that large amount of uncertainties (> 2 mm/day) exists in precipitation projections in RCP4.5 scenario over northern Pakistan and adjoining Jammu and Kashmir.

3.5. GFDL_ESM2G model

For a detailed examination of the climate projection, in this section, projected output of only one model is discussed. The GFDL_ESM2G model has been chosen for the purpose as this model has the least increase in temperature during mid-21st century in RCP4.5 scenario as seen in Fig. 3. Moreover, for dynamic downscaling purpose, the entire simulation data at 6hrly resolution for this model was collected.

Temperature (Tas) difference between present (2001 to 2005) and future climate (2051 to 2055) from GFDL_ESM2G model for RCP4.5 and RCP8.5 scenarios have been plotted in Fig. 10. Seasonally averaged temperature differences for RCP 4.5 scenario are shown in Fig. 10(a–d). Similar plots for RCP8.5 are shown in Fig. 10(e–h). In RCP4.5 scenario, the model shows a reduction in temperature over Rajasthan and adjoining region. Over the study region, no large change in temperature is expected. In this scenario, about 0.5 to 1.5 °C rise is possible in other seasons except in JJAS when the temperature rise will be about 2 °C. Magnitude of temperature increase is more in RCP8.5 scenario. The difference is expected to be more than 1° in almost over the entire region. In JJAS and OND, temperature rise will be 2 to 3 °C over north India and the Himalayan region. In JF, however, the northern parts of India will have a rise of 0.5 to 1 °C in mid-century compared to the present climate. Fig. 11 has the precipitation projections for the two scenarios as in Fig. 10 for temperature. It can be seen that the precipitation climate simulated by the GFDL_ESM2G is characteristically different from the ensemble mean. This model simulates reduction in precipitation in JF and MAM in both RCP4.5 and RCP8.5 scenarios. As most of the precipitation in winter and spring is in the form of snow, this study implies that there will be reduction in snowfall in mid-century over the study region of the Himalayas. In JJAS, over most of

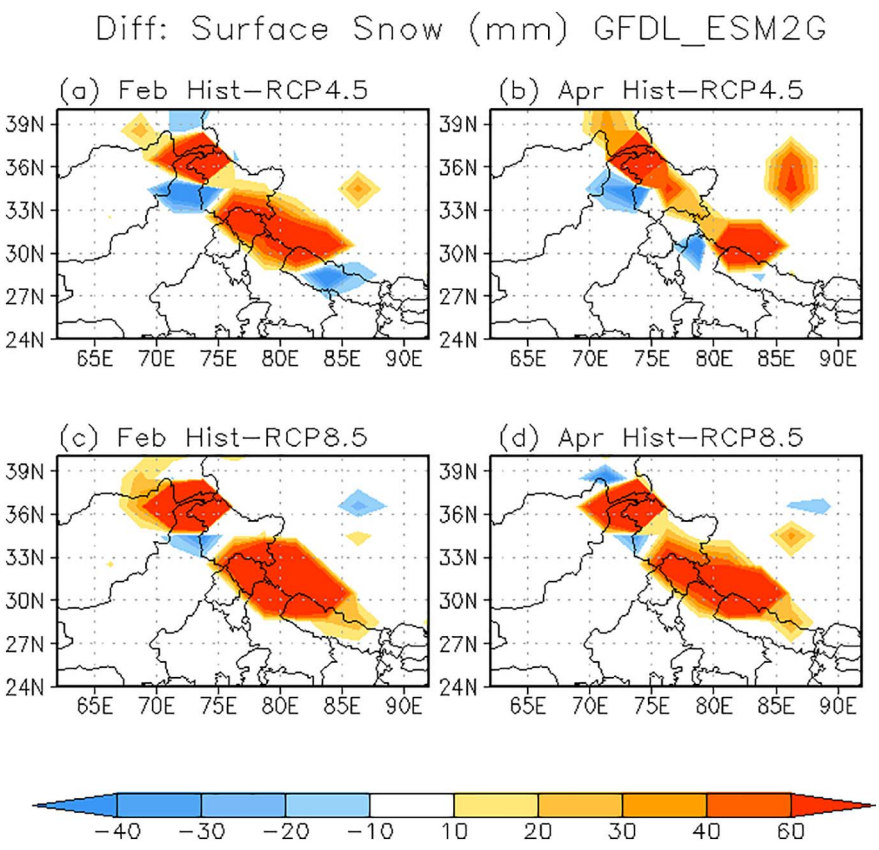

Fig. 12. Difference in accumulated snow on the surface (mm) between present climate (2001–2005) and mid-21st century projections (2051–2055) for the GFDL_ESM2G model (a) end of February, (b) end of April for RCP4.5 scenario (c) end of February and (d) end of April for RCP8.5 scenario.

Gangetic plains, precipitation will also be reduced. In OND, however, precipitation amount is likely to increase in both the scenarios. This increase will be in the range of 0.4 to 1.2 mm/day. This implies that there may be prolonged monsoon season in coming years.

Surface accumulated snow amount from the GFDL_ESM2G model has been examined from historical simulations for RCP4.5 and RCP8.5 projections over the western Himalayan region. This parameter is crucially important for snowmelt runoff and feeding the vast number of rivers originating in the Himalayas including Satluj River. The differences of snow amount between historical run (averaged from 2001 to 2005) and projection runs (averaged from 2051 to 2055) are shown in Fig. 12. While Fig. 12(a and d) shows the accumulated snow difference (mm) at the end of February, Fig. 12(b and d) show the plots for the snow amount at the end of April. It is seen that in mid-century, snow amount by the end of February would be less by about 40–60 mm over most parts of south Kashmir, Himachal Pradesh and Uttarakhand in RCP4.5 scenario as compared to present climate. In RCP8.5 scenario, the reduction will be far greater (> 40 mm). As most of snow starts to melt in spring season, the difference for end-of-April snow indicates that more amount of snow would melt in future climate than the present one. In this case too, available snow amount on the surface would be 30–40 mm less than present climate in RCP8.5 and the difference amount would be 20–30 mm in RCP4.5 scenario. A small area over northern Pakistan and central Nepal region will have more snow amount in RCP4.5 by the end of February as compared to the present climate. However, this increased snow will diminish in RCP8.5 runs. This reduction in snow amount is consistent with rise in surface temperature as seen in Fig. 10.

It is not only that the surface temperature creates a conducive condition for enhanced snowmelt, the upper air conditions will also change in global warming era and annual cycle of snowfall (solid precipitation) would change. Area averaged snowfall (mm/day) for the Satluj basin region (Region-1) has been plotted in Fig. 13a for each month (averaged for the period 2001 to 2005, and 2051–2055 for the historical run, as well as for RCP4.5 and RCP8.5 scenarios. A shift in the snowfall annual cycle is clearly evident in the figure. The peak in the snowfall over the study region occurs in February in historical run. This peak shifts to March in RCP4.5 and prolong from March to April in RCP8.5 runs. Similarly, the onset of snow over this region is delayed to October and November respectively in RCP4.5 and RCP8.5. Evaporation is one of the important components of hydrological cycle and precipitation as well as temperature change impact this variable. Fig. 13b shows the annual cycle of the area averaged evaporation (mm/day) for the Satluj basin region (averaged for the period 2001 to 2005, and 2051–2055) for the historical run, as well as for RCP4.5 and RCP8.5 scenarios. It is seen that global warming on evaporation in the study region will be marginal. However, major shift in maxima and minima of evaporation is noticed. A peak in evaporation seen in May in historical run would occur early in April in RCP8.5 scenario. It is projected that in future climate, June and July will experience more evaporation in RCP8.5 as compared to in August and September in historical simulation. Fig. 13c shows the annual cycle of surface temperature for the two scenarios along with that of historical period. Consistent enhancement of surface temperature in every month is expected in RCP4.5 and RCP8.5 as compared to present climate period. However, there is no shift in the temperature annual cycle with peak temperature seen in Northern Hemisphere summer months.

4. Dynamic downscaling using WRF model

The GFDL_ESM2G model is too coarse to resolve the sharp orography gradient of the Satluj River basin. Therefore, the historical, RCP4.5 and RCP8.5 simulations have been downscaled using triple nested configuration of the WRF model as shown in Fig. 14. The Satluj basin has been resolved using the model at 8 km resolution following Tiwari et al. (2017b). The WRF model has been run for present climate

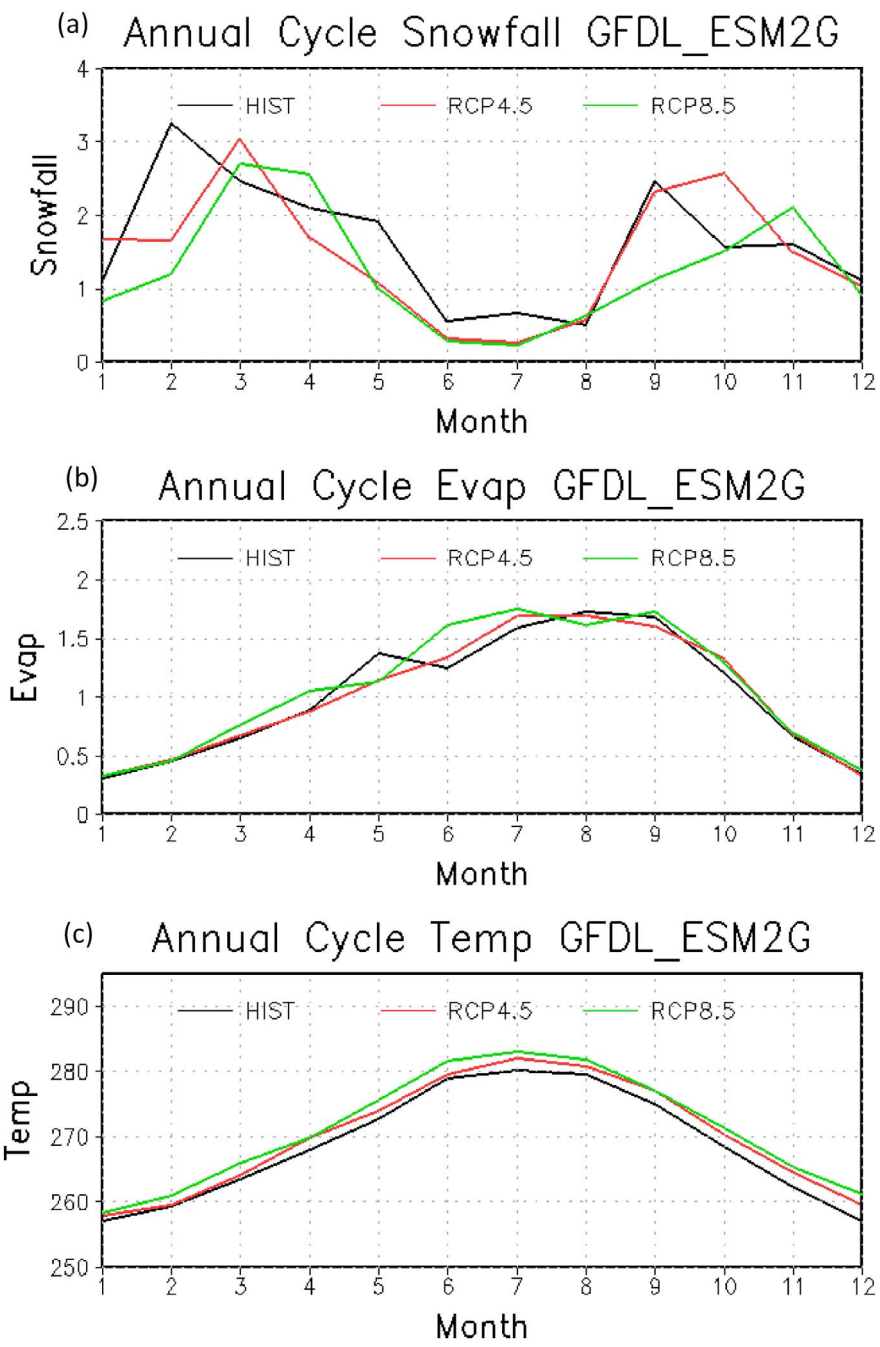

Fig. 13. Annual cycle over Region-1 from GFDL_ESM2G model for runs with historical forcing (2001–2005), RCP4.5 and RCP8.5 forcing (2051–2055) (a) snowfall (mm/day); (b) evaporation (mm/day) and (c) surface sir temperature.

period for 5 years (2001–2005) and future climate projections for 5 years each for RCp4.5 and RCP8.5 scenarios for the period 2051 to 2055.

Temperature (Tas) difference between present climate and future climate from the WRF model has been plotted in Fig. 15. Seasonally averaged temperature differences for RCP 4.5 scenario are shown in Fig. 15(a–d). Similar plots for RCP8.5 are shown in Fig. 15(e–h). During JF, the WRF model simulates warmer temperatures (0.5 to 1.0 °C) during 2051 to 2055 as compared to present climate period (2001–2005) over the most parts of the Satluj basin in RCP4.5 while the temperatures in RCP8.5 are warmer by 1.5 to 2 °C. A small region on the western side of the basin (the plain region) will experience no much change in temperature in RCP4.5 scenario. The difference between the temperatures simulated by the WRF model in MAM is similar to that in JF. The basin will experience about 1 °C warmer climate in mid-21st century in RCP4.5 scenario which is projected to increase up to 1.5 and 2 °C in RCP8.5. The eastern parts of the basin including the region in Tibet will be warmer by > 1.5 °C. Temperature difference between present and future will be similar in JJAS to that in MAM over the most parts of Satluj basin in both RCP4.5 and RCP8.5. The western parts of the basin will be warmer in JJAS than in MAM or JF. The warming is expected to be between 1.5 and 2 °C in RCP8.5. Over the eastern parts of the basin, the temperature rise is expected to be between 1.0 and 1.5 °C in RCPR.5. During OND, while the northern and eastern parts of the basin will be warmer by > 1.5 °C in RCP4.5, it will be more than 2 °C in RCP8.5 scenario. It may be noted here that GFDL-ESM2G model also simulates similar differences in its simulations for this period. However, the global model does not simulate much change in RCP4.5

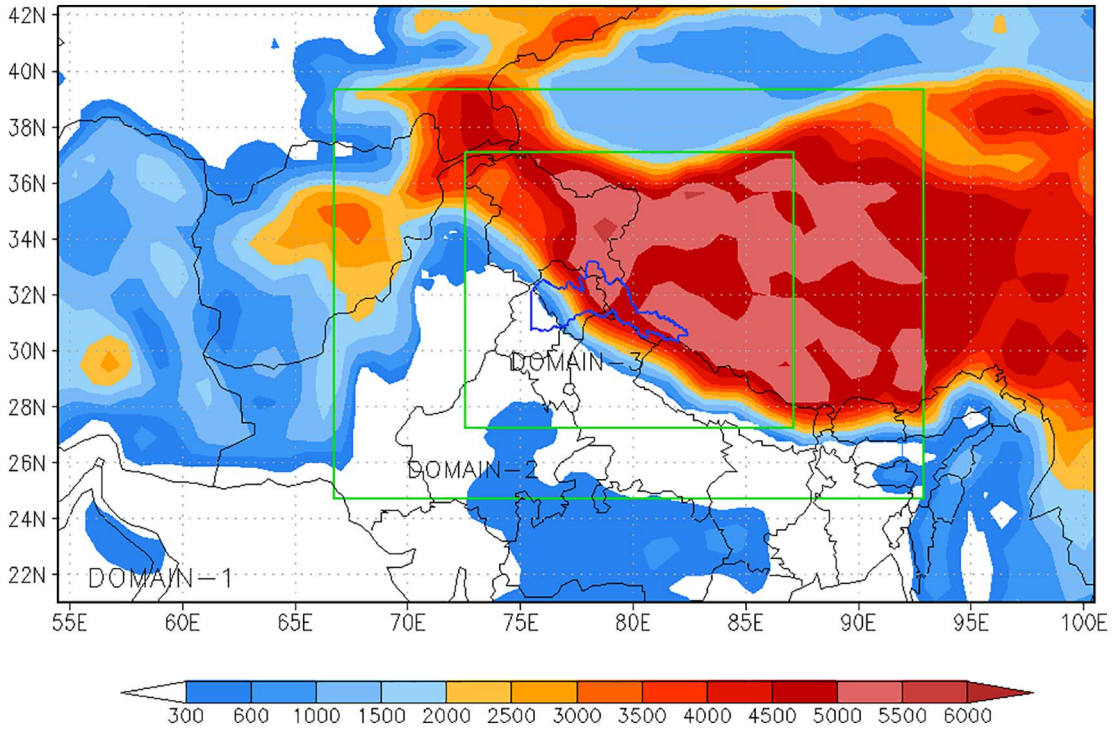

Fig. 14. The WRF model domain for downscaling studies. The three nested domains are marked as rectangular boxes. Mountain topography is shaded in the figure.

scenario compared to present climate than that seen in downscaled runs. Over the Satluj basin area, the global model simulates > 3 °C warming in OND in RCP8.5 scenario. However, the WRF model does not simulate that large difference.

Precipitation differences between present (2001 to 2005) and future climate (2051 to 2055) from the WRF model for RCP4.5 and RCP8.5 scenarios are shown in Fig. 16 for RCP4.5 and RCP8.5 scenarios. No large change in precipitation is seen in JF except increase of about 0.5 mm/day of precipitation in the central parts in the basin in RCP4.5. The precipitation difference in both the future scenarios compared to present climate has a northwest-southwest pattern. It may be noted that the global model (GFDL-ESM2G) has projected a reduction in precipitation in future scenarios as compared to present climate. However, in the downscaling experiment, though differences are not large, an increase in precipitation is seen. Major differences in precipitation simulation from present climate are seen in MAM, JJAS and OND in the WRF model simulations. Similar to JF, a northwest-southeast band of precipitation difference in central parts of the river basin is seen in MAM in both RCP4.5 and RCP8.5 as compared to historical run. The reduction of precipitation is expected to be > 3–6 mm/day in MAM in RCP4.5. However, in RCP8.5 case, the model simulates an increase in precipitation of about 1 to 1.5 mm/day. In contrast, the global model did not simulate such change in precipitation during MAM. In JJAS, the WRF model simulation for the RCP4.5 case indicates areas of both enhanced and reduced precipitation in the basin, while for the RCP8.5 scenario, the model simulates reduced precipitation over most area of the basin. For JJAS, both the global model and the WRF model simulations are mostly consistent with each other. In OND, it is projected that the western parts of the basin will experience enhanced precipitation in RCP4.5. Therefore, the WRF model projections indicate that except in JF, temperature will rise over the entire Satluj basin during 2051–2055 as compared to 2001 to 2005. However, this rise will not be uniform for the two scenarios considered here. Precipitation amount may marginally increase in JF will greatly reduce JJAS in mid-21st century.

5. Streamflow simulations using SWAT model

In order to examine the impact of climate change on the discharge and streamflow of Satluj basin, the SWAT model has been used to simulate the Satluj discharge for the present climate of the years 2001–2005 and for future climate of years 2051–2055 using GFDL_ESM2G precipitation and temperature data. This model was earlier used to simulate discharge in Satluj using observed precipitation and temperature forcing and was found to be reproducing the observed discharge for the year 1982 to 2004 (Tiwari et al., 2017c). The model parameters for the present study were the same as the calibrated run described in Tiwari et al. (2017c). Total number of sub-basins chosen is 32 for hydrological analysis. Fig. 17a shows the simulated discharge using historical runs (2001–2005) as well as the observed discharge at Satluj (entry to Bhakra reservoir). It is seen that global model data is able to capture peak discharge period in JJAS in historical runs. However, the simulated discharge during later part of the monsoon seasons is more. The simulated discharge plots for the future projection period under RCP4.5 and RCP8.5 are shown in Fig. 17b. It is noticed that more amount of discharge also occurs during winter season (JF) in addition to monsoon seasons. However, total annual discharge from Satluj is less than present climate. In Satluj basin, there are two discharge periods- one is in spring (MAM) and other in monsoon season (JJAS) due to spring snowmelt and monsoon precipitation respectively. Discharge peaks are more prominent in RCP8.5 scenario. From Fig. 17b, it is also seen that during 2051–2055, discharge will be less in the peak discharge season (JJAS). There will be some discharge peaks which will be more prominent with larger magnitude. These will also be for shorter period.

Global model data has very coarse resolution and over Satluj basin and only two grid points were available at which data for the precipitation and temperature could be used in the SWAT model. In order to get a proper estimate of discharge in this basin, global model data has to be downscaled at sub-basin level to see the discharge pattern in future climate. The downscaled data from the WRF model described in the previous section provided new dataset of temperature and

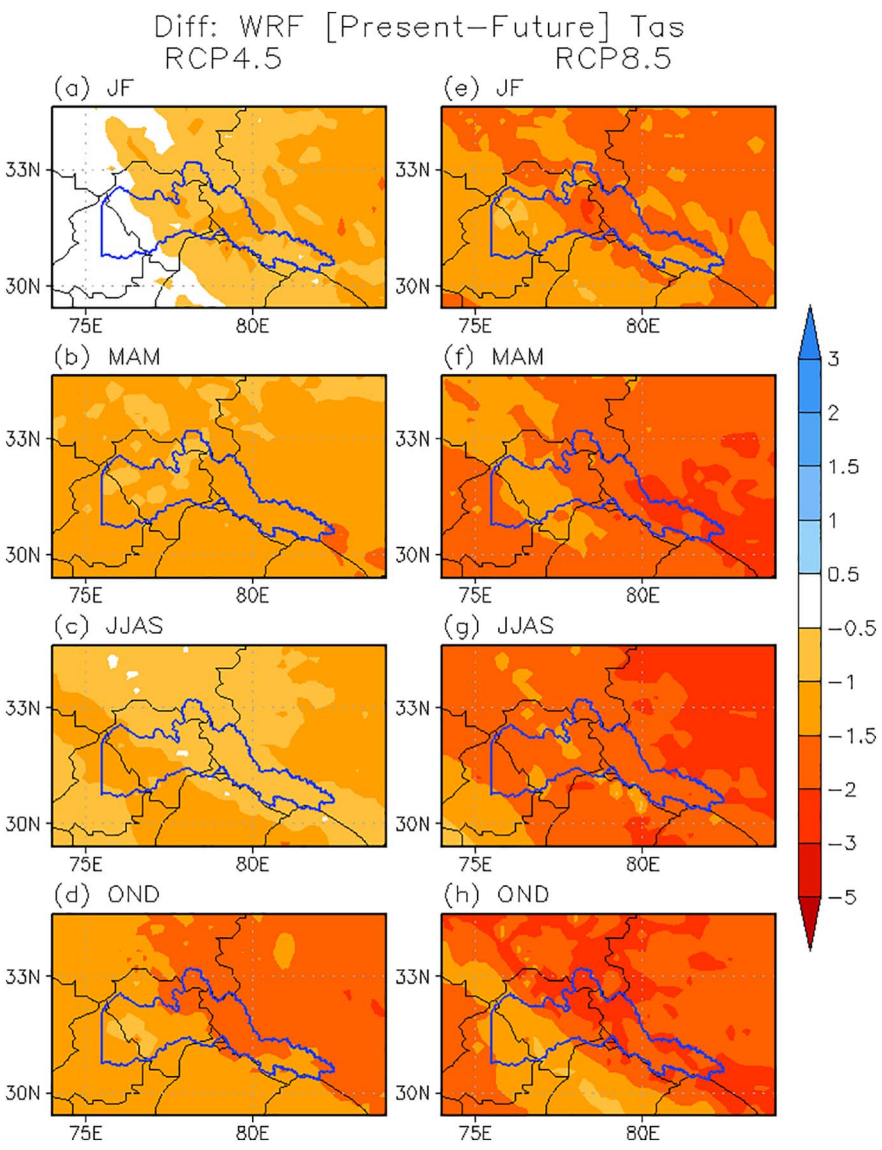

Fig. 15. Difference in surface air temperature (°C) between present climate (2001 to 2005) and mid-21st century projections (2051 to 2055) for the downscaled projection using WRF model (a) January, February (JF), (b) March to May (MAM), (c) June to September (JJAS) and (d) October to December (OND) in RCP4.5 scenario; (e) January February (JF), (f) March to May (MAM), (g) June to September (JJAS) and (h) October to December (OND) in RCP8.5 scenario.

precipitation at very high resolution of 8 km. Using this new high resolution data, the SWAT model has been used to simulate the streamflow of Satluj River for the present climate period (2001–2005) and future climate period (2051–55). The simulated discharge from the SWAT models for these three five-year period are shown in Fig. 17c. It can be seen that in the present climate, peak discharge period is from May to September. It is noticed that in mid-century (2051–2055) under RCP4.5 scenario, the peak discharge period will shift by one month and it will be during June to September. It is also seen that overall discharge amount will be less as compared to present climate (Fig. 17c). The same conclusion is also drawn for RCP8.5 scenario. During winter seasons in historical period as well as in RCP4.5 scenario, the discharge amount is close to zero. However, in RCP8.5 scenario, more discharge amount is seen as compared to RCP4.5 in all the five years. In both RCP4.5 and RCP8.5 scenarios, more amount of short period discharge will be observed which is not seen in historical forcing run. The model precipitation and temperatures lead to an increase in discharge in Satluj River during mid-21st century as compared to present climate. This result is in contrast to the conclusion drawn from the global model results. This is because the WRF model has simulated more precipitation from October to March for various scenarios over the Satluj basin than the present climate as compared to the global model (Fig. 16). This enhanced precipitation in winter period increases melt in spring months.

6. Conclusions

The Himalayan climate system is sensitive to global warming and climate change. In a climate change scenario, variations in snow and glacier melt in the region may alter the regional hydrology and the downstream water flow in the river system. This study attempts to document the mid-21st century climate projections over western Himalayas from some of the CMIP5 global climate models. All the global climate models used in the present analysis indicate that in RCP4.5 scenario, the study region would be warmer by mid-century. Increasing temperature trend in GFDL_ESM2G model projections is minimum for the study area (Region-1). However, precipitation has large interannual variation and large inter-model variation with no large trend.

Statistical significance of the trend has been carried out Mann Kendall trend analysis test for the period from 2000 to 2060. It is found that the temperature trends from all the models studied here are statistically significant at 95% confidence interval. Issue of stationarity in the future climate projections has been addressed by carrying out

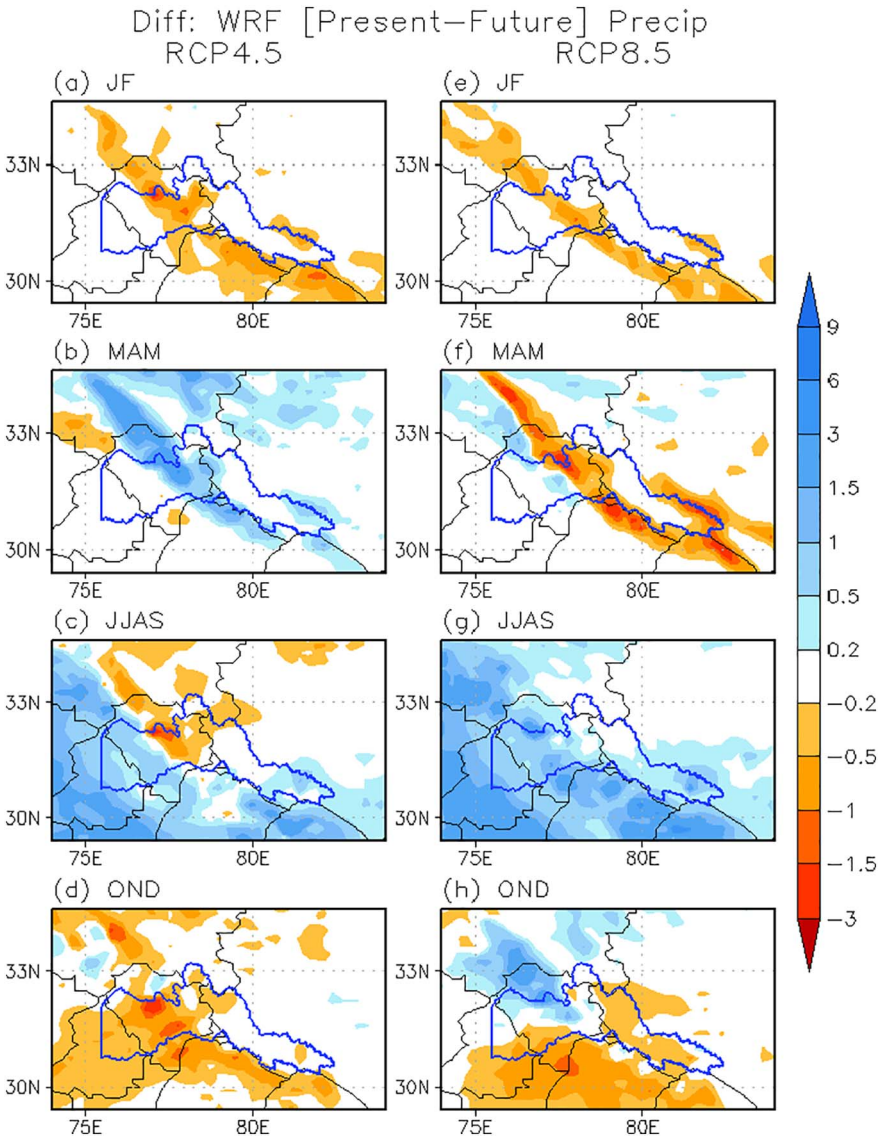

Fig. 16. Same as Fig. 15 but for precipitation (mm/day).

augmented Dickey-Fuller test and KPSS tests on the GFDL_ESM2G model products. The results vary according to scenario chosen and different regions considered.

It is found that while the multi-model ensemble mean simulations of temperature and precipitation with historical forcing for the period 2001–2005 are reasonable, there are large differences among the models in their projections of future climate. The inter-model spread ranges from about 1.5 °C to 5 °C over various areas of the study region in all the seasons. Spread in precipitation projections lies between 0.3 and 1 mm/day in all the seasons except in JJAS when the spread is > 3 mm/day along the Gangetic plains and foothill of Himalayas. It is projected that in mid-century, snow amount by the end of February would be less by about 30–40 mm (RCP4.5 scenario) and about 50 mm (RCP8.5 scenario) over most parts of south Kashmir, Himachal Pradesh and Uttarakhand as compared to present climate. Major shift in the timing of evaporation maxima and minima is noticed. It is projected that in future climate, June and July will experience more evaporation in RCP8.5 as compared to that seen in August and September in historical simulation.

The GFDL_ESM2G model products have been downscaled to Satluj River basin using WRF model and impact of climate change on streamflow has been studied. A northwest-southeast band of precipitation difference in central parts of the river basin is seen in both RCP4.5 and RCP8.5 as compared to historical run. The reduction of precipitation is expected to be > 3–6 mm/day in JJAS for RCP8.5 scenario. During JF and OND, precipitation amount over Satluj River basin shall increase by mid-21st century. The downscaled products suggest that temperature will rise over Satluj basin in 2051–2055 as compared to 2001–2005.

In order to examine the impact of climate change on the discharge and streamflow of Satluj basin, the SWAT model has been used to simulate the Satluj discharge for the present and future climate using GFDL_ESM2G precipitation and temperature data as well as the WRF model downscaled data. The computations show that total annual discharge from Satluj will be marginally more in future than that in present climate, especially in spring season (MAM). Discharge peaks are more prominent in RCP8.5 scenario.

It may be noted here that downscaling methods also add uncertainty to climate simulations due to the limitations inherent in the technique. Physical parameterization of various sub-grid scale processes in the regional climate model can strongly influence biases and skill of the model (e.g., Kjellström and Giorgi, 2010; Sinha et al., 2013; Tiwari et al., 2017b). In addition to the uncertainties in downscaling, the global models themselves also contribute to uncertainties in the

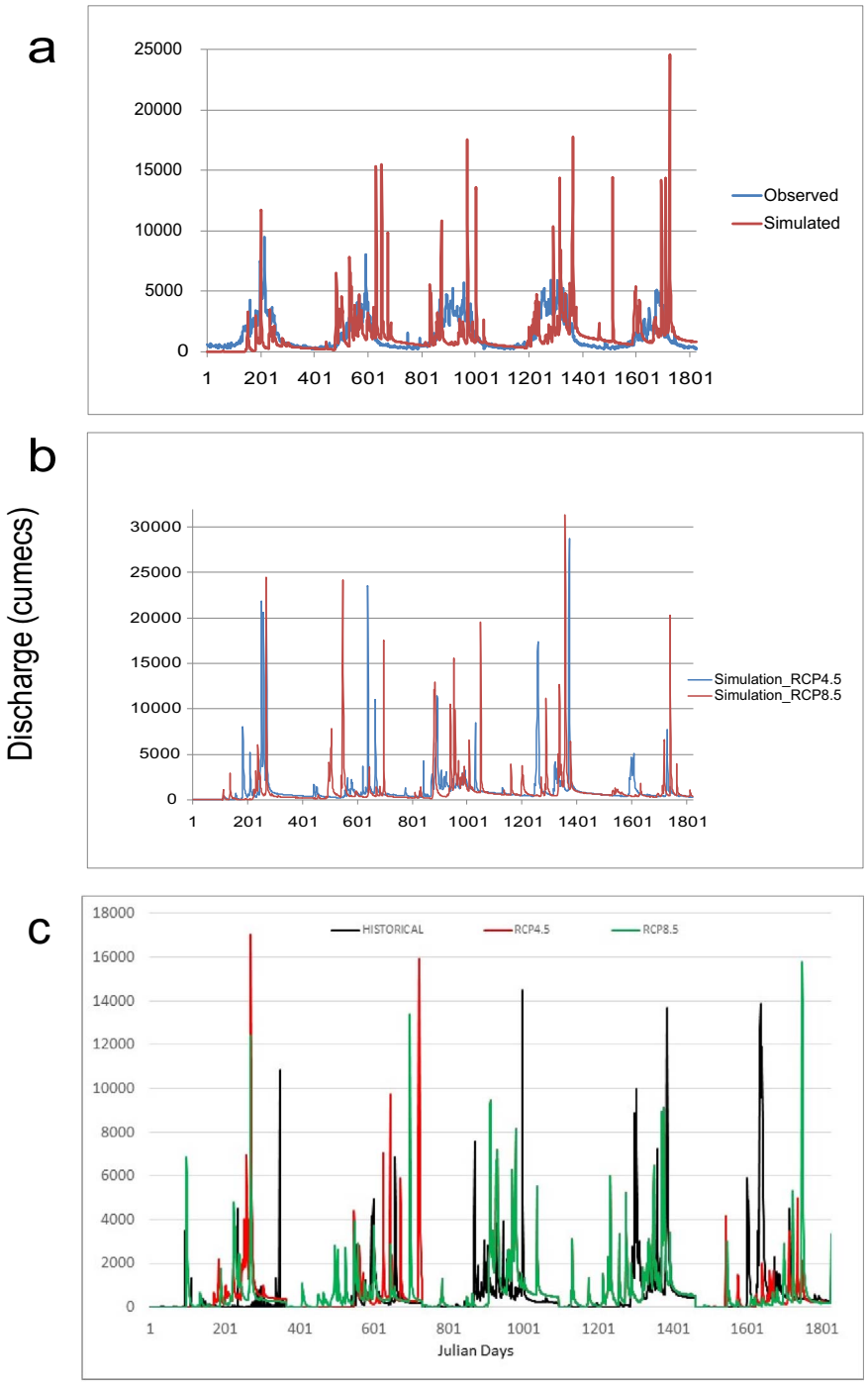

Fig. 17. Simulated discharge from Satluj River using SWAT model with GFDL_ESM2G meteorological forcing for (a) Historical (2001–2005) and observed discharge; (b) RCP4.5 (2051–2055); and (c) downscaled GFDL_ESM2G (using WRF model) With Historical (2001–2005) and future climate (2051–2055) under RCP4.5 and RCP8.5 scenarios.

projections by providing contrasting projections. While analyzing the results, care has been taken to describe only those findings which are robust.

Acknowledgement

This work was carried out as a part of “Modeling of Changing Water Cycle and Climate” project of Ministry of Earth Sciences, Government of India.

References

Barnett, T.P., Adam, J.C., Lettenmaier, D.P., 2005. Potential impacts of a warming climate on water availability in snow-dominated regions. Nature 438, 303–309.

Beniston, M., 2003. Climatic change in mountain regions: a review of possible impacts. Clim. Chang. 59, 5–31.

Bhutiyani, M.R., Kale, V.S., Pawar, N.J., 2007. Long-term trends in maximum, minimum and mean annual air temperatures across the Northwestern Himalaya during the twentieth century. Clim. Chang. 85, 159–177.

Bhutiyani, M.R., Kale, V.S., Pawar, N.J., 2008. Changing stream- flow patterns in the rivers of northwestern Himalaya: implications of global warming in the 20th century. Curr. Sci. India 95 (5), 618–626.

Bhutiyani, M.R., Kale, V.S., Pawar, N.J., 2010. Climate change and the precipitation variations in the Northwestern Himalaya: 1866–2006. Int. J. Climatol. 30, 535–548.

Buytaert, W., 2012. Assessment of the impacts of climate change on mountain hydrology: development of a methodology through a case study in the Andes of Peru. Mt. Res. Dev. 32, 385–386.

Chaturvedi, R.K., Joshi, J., Jayaraman, M., Bala, G., Ravindranath, N.H., 2012. Multi-model climate change projections for India under representative concentration pathways. Curr. Sci. 103, 791–802.

Chen, F., Dudhia, J., 2000. Coupling an advanced land-surface/hydrology model with the Penn State/NCAR MM5 modeling system. Part I: model description and

implementation. Mon. Weather Rev. 129, 569–585.
Christensen, N., Wood, A., Voisin, N., Lettenmaier, D., Palmer, R., 2004. Effects of climate change on the hydrology and water resources of the Colorado River Basin. Clim. Chang. 62, 337–363.
Collins, W.J., Bellouin, N., Doutriaux-Boucher, M., Gedney, N., Halloran, P., Hinton, T., Hughes, J., Jones, C.D., Joshi, M., Liddicoat, S., Martin, G., O'Connor, F., Rae, J., Senior, C., Sitch, S., Totterdell, I., Wiltshire, A., Woodward, S., 2011. Development and evaluation of an Earth-system model—HadGEM2. Geosci. Model Dev. 4, 1051–1075. http://dx.doi.org/10.5194/gmd-4-1051-2011.
Dash, S.K., Mishra, S.K., Pattnayak, K.C., Mamgain, A., Mariotti, L., Coppola, E., Giorgi, F., Giuliani, G., 2014. Projected seasonal mean summer monsoon over India and adjoining regions for the twenty-first century. Theor. Appl. Climatol. 122 (3), 581–593.
Dickey, D.A., Fuller, W.A., 1979. Distribution of the estimators for autoregressive time series with a unit root. J. Am. Stat. Assoc. 74, 423–431.
Divya, Mehrotra, R., 1995. Climate change and hydrology with emphasis on the Indian subcontinent. Hydrol. Sci. J. 40, 231–242.
Dunne, J.P., John, J.G., Shevliakova, E., Stouffer, R.J., Krasting, J.P., Malyshev, S.L., et al., 2013. GFDL's ESM2 global coupled climate–carbon earth system models. Part II: carbon system formulation and baseline simulation characteristics. J. Clim. 26, 2247–2267. http://dx.doi.org/10.1175/JCLI-D-12-00150.1.
Elshamy, M.E., Seierstad, I.A., Sorteberg, A., 2009. Impacts of climate change on Blue Nile flows using bias-corrected GCM scenarios. Hydrol. Earth Syst. Sci. 13, 551–565.
Eriksson, M., Jianchu, X., Shrestha, A.B., Vaidya, R.A., Nepal, S., Sandstrom, K., 2009. The Changing Himalayas: Impact of Climate Change on Water Resources and Livelihoods in the Greater Himalayas, Kathmandu. International Centre for Integrated Mountain Development (ICIMOD).
Fowler, H.J., Blenkinsop, S., Tebaldi, C., 2007. Linking climate change modelling to impacts studies: recent advances in downscaling techniques for hydrological modelling. Int. J. Climatol. 27 (12), 1547–1578. http://dx.doi.org/10.1002/joc.1556.
Gosain, A.K., Rao, S., Basuray, D., 2006. Climate change impact assessment on hydrology of Indian river basins. Curr. Sci. 90 (3), 346–353.
Grell, G., Devenyi, D., 2002. A generalized approach to parameterizing convection combining ensemble and data assimilation techniques. Geophys. Res. Lett. 29, 1693–1697.
Hall, D.K., Riggs, G.A., Salomonson, V.V., 2006. MODIS/Terra Snow Cover 5-Min L2 Swath 500 m. Version 5. NASA National Snow and Ice Data Center Distributed Active Archive Center, Boulder, Colorado USA. http://dx.doi.org/10.5067/ACYTYZB9BEOS.
Harris, I., Jones, P.D., Osborn, T.J., Lister, D.H., 2014. Updated high-resolution grids of monthly climatic observations. Int. J. Climatol. http://dx.doi.org/10.1002/joc.3711. (in press).
Hong, S.Y., Lim, J., 2006. The WRF single-moment 6-class microphysics scheme (WSM6). J. Kor. Meteorol. Soc. 42, 129–151.
Hong, S.Y., Pan, H.L., 1996. Nonlocal boundary layer vertical diffusion in a medium range forecast model. Mon. Weather Rev. 124 (10), 2322–2339.
Immerzeel, W.W., Pellicciotti, F., Bierkens, M.F.P., 2013. Rising river flows throughout the twenty-first century in two Himalayan glacierized watersheds. Nat. Geosci. 6, 1–4. http://dx.doi.org/10.1038/ngeo1896.
IPCC, 2013. Summary for policymakers. In: Climate Change 2013: The Physical Science Basis. Contribution of Working Group I to the Fifth Assessment Report of the Intergovernmental Panel on Climate Change. Cambridge University Press, Cambridge, United Kingdom and New York, NY, USA.
Jones, P.D., Lister, D.H., Osborn, T.J., Harpham, C., Salmon, M., Morice, C.P., 2012. Hemispheric and large-scale land-surface air temperature variations: an extensive revision and an update to 2010. J. Geophys. Res. 117, D05127. http://dx.doi.org/10.1029/2011JD017139.
Kjellström, E., Giorgi, F., 2010. Introduction. Clim. Res. 44, 117–119.
Knutti, R., Furrer, R., Tebaldi, C., Cermak, J., Meehl, G.A., 2010. Challenges in combining projections from multiple climate models. J. Clim. 23, 2739–2758.
Kwiatkowski, D., Phillips, P.C.B., Schmidt, P., Shin, Y., 1992. Testing the null of stationarity against the alternative of a unit root: how sure are we that economic time series have a unit root? J. Econ. 54, 159–178.
Lo, J.C.-F., Yang, Z.-L., Pielke Sr., R.A., 2008. Assessment of three dynamical climate downscaling methods using the weather research and forecasting (WRF) model. J. Geophys. Res. 113, D09112. http://dx.doi.org/10.1029/2007JD009216.
Martin, G.M., Bellouin, N., Collins, W.J., Culverwell, I.D., Halloran, P.R., Hardiman, S.C., Hinton, T.J., Jones, C.D., McDonald, R.E., McLaren, A.J., O'Connor, F.M., Roberts, M.J., Rodriguez, J.M., Woodward, S., Best, M.J., Brooks, M.E., Brown, A.R., Butchart, N., Dearden, C., Derbyshire, S.H., Dharssi, I., Doutriaux-Boucher, M., Edwards, J.M., Falloon, P.D., Gedney, N., Gray, L.J., Hewitt, H.T., Hobson, M., Huddleston, M.R., Hughes, J., Ineson, S., Ingram, W.J., James, P.M., Johns, T.C., Johnson, C.E., Jones, A., Jones, C.P., Joshi, M.M., Keen, A.B., Liddicoat, S., Lock, A.P., Maidens, A.V., Manners, J.C., Milton, S.F., Rae, J.G.L., Ridley, J.K., Sellar, A., Senior, C.A., Totterdell, I.J., Verhoef, A., Vidale, P.L., Wiltshire, A., 2011. The HadGEM2 family of met office unified model climate configurations. Geosci. Model Dev. 4 (3), 723–757. http://dx.doi.org/10.5194/gmd-4-723-2011.
Milly, P.C.D., Betancourt, Julio, Falkenmark, Malin, Hirsch, Robert M., Kundzewicz, Zbigniew W., Lettenmaier, Dennis P., Stouffer, Ronald J., 2008. Stationarity is dead: whither water management? Science 319 (5863), 573–574. http://dx.doi.org/10.1126/science. 1151915.
Mitchel, T.D., Jones, P.D., 2005. An improved method of constructing a database of monthly climate observations and associated high-resolution grids. Int. J. Climatol. 25, 693–712. http://dx.doi.org/10.1002/Joc.1181.
Moss, R.H., Edmonds, J.A., 2010. The next generation of scenarios for climate change research and assessment. Nature 463, 747–756.
New, M., Hulme, M., Jones, P.D., 2000. Representing twentieth century space-time climate variability. Part 2: development of 1901–96 monthly grids of terrestrial surface climate. J. Clim. 13, 2217–2238.
New, M., Todd, M., Hulme, M., Jones, P., 2001. Precipitation measurements and trends in the twentieth century. Int. J. Climatol. 21 (15), 1889–1922. http://dx.doi.org/10.1002/joc.680.
Nogués-Bravo, D., Araújo, M.B., Errea, M.P., Martínez-Rica, J.P., 2007. Exposure of global mountain systems to climate warming during the 21st century. Glob. Environ. Chang. 17, 420–428.
Palazzi, E., von Hardenberg, J., Provenzale, A., 2013. Precipitation in the Hindu-Kush Karakoram Himalaya: observations and future scenarios. J. Geophys. Res. Atmos. 118, 85–100.
Pattnayak, K.C., Panda, S.K., Saraswat, Vaishali, Dash, S.K., 2013. Relationship between tropospheric temperature and Indian summer monsoon rainfall as simulated by RegCM3. Clim. Dyn. 2016 (46), 3149–3162.
Pattnayak, K.C., Kar, S.C., Mamta, Dalal, Pattnayak, R.K., 2017. Projections of annual rainfall and surface temperature from CMIP5 models over the BIMSTEC countries. Glob. Planet. Chang. http://dx.doi.org/10.1016/j.gloplacha.2017.03.005.
Randall, D.A., Wood, R.A., Bony, S., Colman, R., Fichefet, T., Fyfe, J., Kattsov, V., Pitman, A., Shukla, J., Srinivasan, J., Stouffer, R.J., Sumi, A., Taylor, K.E., 2007. Climate models and their evaluation. In: Solomon, S. (Ed.), Climate Change 2007: The Physical Science Basis. Contribution of Working Group I to the Fourth Assessment Report of the Intergovernmental Panel on Climate Change. Cambridge University Press, Cambridge, UK.
Schmidt, G.A., Kelley, M., Nazarenko, L., Ruedy, R., Russell, G.L., Aleinov, I., Bauer, M., Bauer, S.E., Bhat, M.K., Bleck, R., Canuto, V., Chen, Y.-H., Cheng, Y., Clune, T.L., Del Genio, A., de Fainchtein, R., Faluvegi, G., Hansen, J.E., Healy, R.J., Kiang, N.Y., Koch, D., Lacis, A.A., LeGrande, A.N., Lerner, J., Lo, K.K., Matthews, E.E., Menon, S., Miller, R.L., Oinas, V., Oloso, A.O., Perlwitz, J.P., Puma, M.J., Putman, W.M., Rind, D., Romanou, A., Sato, M., Shindell, D.T., Sun, S., Syed, R.A., Tausnev, N., Tsigaridis, K., Unger, N., Voulgarakis, A., Yao, M.-S., Zhang, J., 2014. Configuration and assessment of the GISS ModelE2 contributions to the CMIP5 archive. J. Adv. Model. Earth Syst. 6 (1), 141–184. http://dx.doi.org/10.1002/2013MS000265.
Sengupta, A., Rajeevan, M., 2013. Uncertainty quantification and reliability analysis of CMIP5 projections for the Indian summer monsoon. Curr. Sci. 105 (12), 1694–1703.
Singh, P., Bengtsson, L., 2004. Effect of warmer climate on the depletion of snow-covered area in the Satluj basin in the western Himalayan region. Hydrol. Sci. J. 48 (3), 413–425.
Singh, P., Kumar, N., 1997. Impact of climate change on the hydrological response of a snow and glacier melt runoff dominated Himalayan river. J. Hydrol. 193, 316–350.
Sinha, P., Mohanty, U.C., Kar, S.C., Dash, S.K., Kumari, S., 2013. Sensitivity of the GCM driven summer monsoon simulations to cumulus parameterization schemes in nested RegCM3. Theor. Appl. Climatol. 112 (1–2), 285–306. http://dx.doi.org/10.1007/s00704-012-0728-5.
Skamarock, W.C., Klemp, J.B., Dudhia, J., Gill, D.O., Barker, D.M., Wang, W., Powers, J.G., 2005. A description of the advanced research WRF version 2, NCAR technical note. www.wrf-model.org.
Thayyen, R.J., Gergan, J.T., 2010. Role of glaciers in watershed hydrology: a preliminary study of a "Himalayan catchment". Cryosphere 4, 115–128.
Tiwari, P.R., Kar, S.C., Mohanty, U.C., Kumari, S., Sinha, P., Nair, A., Dey, S., 2014. Skill of precipitation prediction with GCMs over north India during winter season. Int. J. Climatol. 34 (12), 3440–3455. http://dx.doi.org/10.1002/joc.3921.
Tiwari, Sarita, Kar, S.C., Bhatla, R., 2015. Examination of snowmelt over Western Himalayas using remote sensing data. Theor. Appl. Climatol. 125, 227–239. http://dx.doi.org/10.1007/s00704-015-1506-y.
Tiwari, Sarita, Kar, S.C., Bhatla, R., 2016a. Interannual variability of snow water equivalent (SWE) over Western Himalayas. Pure Appl. Geophys. 173, 1317–1335. http://dx.doi.org/10.1007/s00024-015-1163-1.
Tiwari, P.R., Kar, S.C., Mohanty, U.C., Dey, S., Sinha, P., Raju, P.V.S., Shekhar, M.S., 2016b. On the dynamical downscaling and bias correction of seasonal-scale winter precipitation predictions over North India. Q. J. R. Meteorol. Soc. 142 (699), 2398–2410.
Tiwari, P.R., Kar, S.C., Mohanty, U.C., Dey, S., Sinha, P., Shekhar, M.S., 2017a. Sensitivity of the Himalayan orography representation in simulation of winter precipitation using regional climate model (RegCM) nested in a GCM. Clim. Dyn. http://dx.doi.org/10.1007/s00382-017-3567-3.
Tiwari, Sarita, Kar, S.C., Bhatla, R., 2017b. Dynamic downscaling over western Himalayas: impact of cloud microphysics schemes. Atmos. Res. http://dx.doi.org/10.1016/j.atmosres.2017.10.007.
Tiwari, Sarita, Kar, S.C., Bhatla, R., Bansal, R., 2017c. Temperature index based snowmelt runoff modelling for Satluj River Basin in the Western Himalayas. Meteorol. Appl. http://dx.doi.org/10.1002/met.1692.
Watanabe, S., Hajima, T., Sudo, K., Nagashima, T., Takemura, T., Okajima, H., Nozawa, T., Kawase, H., Abe, M., Yokohata, T., Ise, T., Sato, H., Kato, E., Takata, K., Emori, S., Kawamiya, M., 2011. MIROC-ESM 2010: model description and basic results of CMIP5-20c3m experiments. Geosci. Model Dev. 4, 845–872. http://dx.doi.org/10.5194/gmd-4-845-2011.
Wilby, R.L., Charles, S.P., Zorita, E., Timbal, B., Whetton, P., Mearns, L.O., 2004. Guidelines for Use of Climate Scenarios Developed From Statistical Downscaling Methods. Supporting Material of the Intergovernmental Panel on Climate Change (IPCC), Prepared on Behalf of Task Group on Data and Scenario Support for Impacts and Climate Analysis (TGICA).